

Review of liquid-based systems to recover low-grade waste heat for electrical energy generation

Chun Cheng¹, Yawen Dai¹, Jie Yu¹, Chang Liu², Sijia Wang², Shien Ping Feng^{2}, Meng Ni^{1*}*

1 Department of Building and Real Estate, The Hong Kong Polytechnic University, Hung Hom, Kowloon, Hong Kong, China

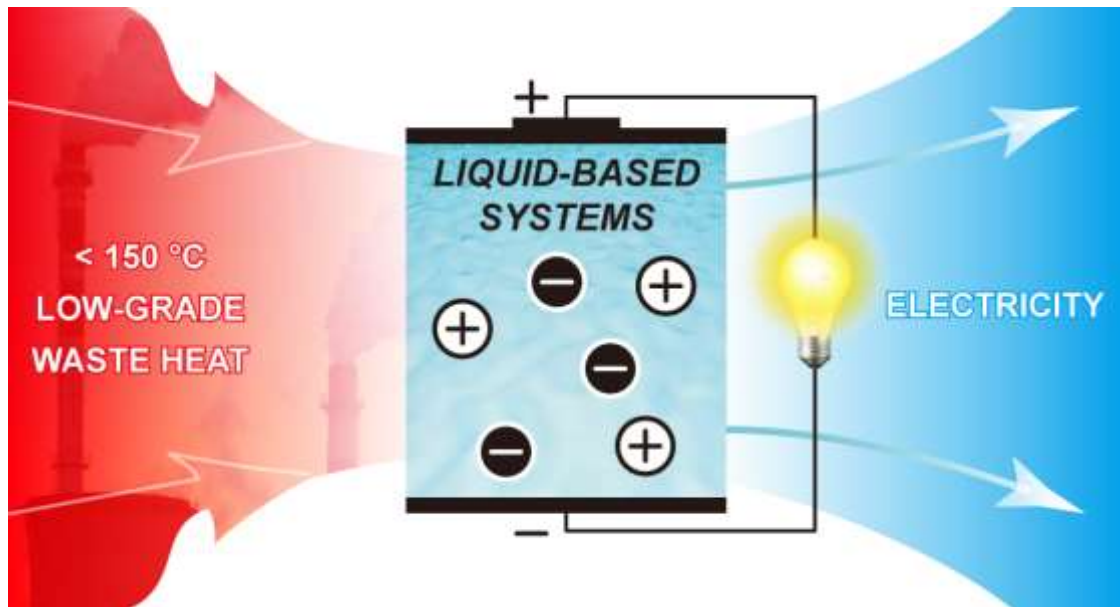
2 Department of Mechanical Engineering, The University of Hong Kong, Pokfulam Road, Hong Kong, China

ABSTRACT

A large amount of low-grade waste heat from the industry has usually been discarded. In order to recover the huge amount of waste heat for a sustainable society, extensive efforts have been made to develop high-performance and low-cost thermoelectric generators based on the Seebeck effect of solid semiconductors. In addition, liquid-based heat-to-electricity systems have been developed and demonstrated a good potential for practical applications. This review aims to provide an overview of the newly developed liquid-based technologies for waste heat recovery, including thermo-electrochemical cells (TECs), thermally regenerative electrochemical cycles (TREC), and thermo-osmotic energy conversion (TOEC) systems. The working principles of these technologies will be introduced and the key factors affecting their performance will be discussed. A perspective to discuss the current challenges and application potential of each system and future research directions will be provided.

Keywords: thermochemistry; low-grade heat; thermo-electrochemical cells; thermally regenerative electrochemical cycles; thermo-osmotic energy conversion.

TOC GRAPHICS



MAIN TEXT

1. Introduction

A huge amount of low-grade heat (<150 °C) from solar thermal, geothermal and industrial facilities is heavily wasted every year. For example, the rejected energy accounted for 67.5% of the total energy consumption of US in 2019.¹ Even worse, a large proportion of waste heat is low-grade heat.² For example, 92.4% of total waste heat from power plants was below 150 °C in 2007.³ Also, all of the waste heat in food processing, and commercial and building sector almost belong to the low-grade waste heat.³ In the UK, thermal energy accounts for 72% of industrial energy consumption and low temperature process accounts for 31%.⁴ Thus, a large amount of waste heat is discarded without utilization. How to effectively and economically recover the low-grade heat is critical to improve the overall energy efficiency and alleviate heat island effects for a sustainable future.

There are two main methods for converting the low-grade waste heat into electrical power. The first one is based on the Seebeck effect of solid semiconductor, or even conducting polymer electrodes (PEDOT-PSS).⁵⁻⁸ The other one mainly relies on the liquid-based entropy change system like temperature-dependent redox couple to use heat as a driving force for power generation. In addition to these two main methods, some researchers recently developed electrochemical sodium heat engines for thermal-to-electric energy conversion, which are on the basis of phase change reactions.^{9,10}

The Seebeck effect was discovered by Thomas Johann Seebeck in the early 19th century. It was found that the magnetic field was generated when connecting two different metal wires with different temperatures being applied to the two nodes. It was explained as thermoelectricity (Seebeck effect). This effect depends on the different thermal responses of different materials, which create potential difference. For example, more holes are formed at the hot end of p-type

semiconductor, creating a hole gradient. As a result, holes tend to diffuse from the high concentration region (hot end) to the low concentration region (cold end) inside the material, establishing a potential difference. When a balance is reached between potential caused current and thermal induced current, a stable voltage can be formed between the two ends. However, the temperature induced voltage of typical thermoelectric (TE) is generally at $\mu\text{V K}^{-1}$ level,⁸ which is much lower than that of thermo-electrochemical cells (TECs) (mV K^{-1}). Moreover, the generated current density is small, leading to a low power density. For example, the reported power density of flexible inorganic Ag_2S -based thermoelectric semiconductor material is only 0.08 W m^{-2} , and the power density of an organic thermoelectric devices is even 2 orders of magnitude lower.¹¹ For comparison, the power density of liquid-based system such as Cu/Zn - TRAFB (copper/zinc bimetallic thermally-regenerative ammonia-based battery) is much higher (280 W m^{-2}).⁹ Additionally, the thermoelectric semiconductor materials require advanced manufacturing process, resulting in a high cost and difficulty in large scale commercial application. The average cost of thermoelectric semiconductor materials is hundreds to thousands of dollars per kilogram, contributing to 50%-80% of the total cost of the semiconductor-based thermoelectric devices.^{13,14} Nowadays, some scientists focus on the thermal photovoltaic conversion to harvest waste heat. The electrical power generated from a broadband blackbody thermal source was demonstrated with a maximum value, i.e. 0.61 W m^{-2} with a temperature difference of $150 \text{ }^\circ\text{C}$.¹¹ The optimization in power density, efficiency and figure of merit is inherently constrained (which will be discussed below in detail) as the intensive properties such as Seebeck coefficient, thermal conductivity and electrical resistivity are often coupled together.

For comparison, the liquid-based system avoids these problems and introduces more possible improvement approaches.

The liquid-based systems rely on redox couples to carry charges in the electrolyte. Several liquid-based novel systems have been recently developed to harvest heat including TECs (thermo-electrochemical cells), TRECs (thermally regenerative electrochemical cycles), thermal regenerative ammonia-based batteries (TRABs), DTCC (direct thermal charging cell) and so on. These cells or cycles are based on early thermogalvanic cells (TGCs) and exhibit the features and merits of galvanic cells such as metal-ion batteries. Specially, TOEC (thermo-osmotic energy conversion) is based on the large salinity differences to generate power, which requires a robust membrane to create a pressurized flux (by a temperature difference) to drive a turbine for electric power generation. TRECs, TOEC, TRABs and DTCC show obvious advantages over other types of thermal-to-electric energy conversion technologies. An excellent review by Yang et al.¹² has summarized the developments in TRECs for low-grade heat conversion. However, the current literature is lacking a systematic review on various liquid-based systems for thermoelectric energy conversion. In this article, we aim to provide a timely literature review on various liquid-based systems for converting low-grade heat into electric energy. Not only TRECs, but also other technologies, such as TOEC, TRABs and DTCC are included. The working principles of different systems are introduced. Their performance and features are summarized and compared. The challenges and future research directions are discussed.

2. Liquid-based systems

In this section, different liquid-based systems including TECs, TRECs, TOEC and so on will be discussed in detail.

2.1 Thermo-electrochemical cells (TECs)

Thermo-electrochemical cells (TECs), consist of anode, cathode, electrolyte and a separator. TECs are non-isothermal electrochemical cell systems. A voltage is established by holding two

electrodes at different temperature within the electrolyte. Electrical current can be produced by connecting the two electrodes. Comparing with the semiconductor-based thermal-electrical conversion technology, the principle of TECs is based on temperature-dependent redox couple. The oxidation and reduction reactions happen on the two electrodes and the oxidized and reduced species transport through the electrolyte. The reactions produce a continuous and stable voltage if there is no degradation of components of TECs. The 3D and 2D schematic representations of TEC are shown in Fig. 1.

The whole energy conversion process is a combination of heat transfer, thermodynamics, electrode kinetics, and mass transfer.¹³ Some parameters derived from solid-state thermoelectric systems have been introduced to the TECs to evaluate the efficiency and performance.

The parameter of thermopower (also called temperature coefficient in TECs or Seebeck coefficient in TE) is the ratio of potential difference to the temperature change, describing the ability of producing voltage per unit temperature difference. Thermopower is an intrinsic property of a material. For TE, it is positive if current flows from hot side to cold side inside the semiconductor, which means the thermopower is positive when the current flow direction in external circuit is opposite to the temperature decreasing direction, the electric field $-dV/dx$ and the temperature gradient dT/dx have the same direction. Therefore, the thermopower of n-type semiconductor is negative while p-type is positive. The thermopower α^* of TE is defined as the ratio of electric field $-dV/dx$ and the temperature gradient dT/dx .¹⁴ And it is given below:

$$\alpha^* = -\frac{dV/dx}{dT/dx} = -\frac{V(T_H)-V(T_L)}{T_H-T_L} \quad (1)$$

where V is the voltage, T_H and T_L are the temperatures of hot side and cold side respectively. For a redox reaction:



The common thermopower α^* calculation equation in most of papers is given below:

$$\alpha^* = \frac{V(T_H) - V(T_L)}{T_H - T_L} = \frac{\Delta S}{nF} \quad (3)$$

where n is the number of transferred electrons of this reaction, F is Faraday's constant, ΔS is entropy change of this reaction. In regardless of Eastman entropies and transported entropies, ΔS is equal to $S_B - S_A$. As the thermopower is related to the entropies, it can indicate the spontaneity of reactions. Taking $\text{Fe}^{2+}/\text{Fe}^{3+}$ redox couple as an example, the entropy is positive up to 1.76 mV K^{-1} .¹⁵

However, the current carriers are ions but not electrons inside TECs. In order to follow the definition of thermopower in TE, as the thermopower is positive when the current flow direction in external circuit is opposite to the temperature decreasing direction, a more appropriate definition is given based on the electric field and temperature gradient. Taking this into consideration, the equation needs to be corrected. The corrected thermopower is as below:

$$\alpha = -\frac{V(T_H) - V(T_L)}{T_H - T_L} = -\frac{\Delta S}{nF} \quad (4)$$

Therefore the thermopower for $\text{Fe}^{2+}/\text{Fe}^{3+}$ redox couple should be -1.76 mV K^{-1} . The Fe^{3+} obtains an electron at the hot side of TECs (cathode) while Fe^{2+} losses an electron at the cold side (anode). The current direction is exactly same to the temperature decreasing direction. When introducing the TE definition into TECs, the p-type electrolyte is with the same direction between electric field and the temperature gradient. So the n-type electrolyte is with positive corrected thermopower, the p-type is with negative corrected thermopower. Briefly, if the hot side is cathode, cold side is anode then it is p-type electrolyte with negative corrected thermopower. The inconsistencies in experimental methods and calculations attribute to the confusion in thermopower data. This paper will provide the original thermopower to show the respect of the authors. The thermopower data of typical redox couples will be given and the p-type or n-type electrolyte will be noted according to the actual situation mentioned in each paper in Table 1.

Table 1Thermopower α of typically different redox couples.

Redox couple	Original thermopower α (mV K ⁻¹)	p/n type*	Electrolyte	Reference
[Fe(CN) ₆] ³⁻ /[Fe(CN) ₆] ⁴⁻	-1.42	n	0.4 M in water	15
[Fe(CN) ₆] ³⁻ /[Fe(CN) ₆] ⁴⁻	4.2	n	24 M urea and 2.6 M GdmCl	26
[Fe(CN) ₆] ³⁻ /[Fe(CN) ₆] ⁴⁻	3.73	n	3 M GdmCl	27
Fe(ClO ₄) ₂ /Fe(ClO ₄) ₃	1.76	p	0.8 M in water	15
I ⁻ /I ₃ ⁻	0.97	n	0.01 M in in ethylammonium nitrate (EAN) ionic liquid	32
Fc, I ₂ /[Fc][I ₃]	1.67	n	30 mM [DiBoylFc][I ₃] in [Emim] [NTf ₂]	77
[Co(py-pz) ₃] ^{2+/3+}	2.36	p	0.1M in 3:1 DMSO:[C ₂ mim][eFAP]	29
[Co(bpy) ₃] ^{2+/3+}	1.21	n	0.05 M [Co(bpy) ₃]Cl ₂ /[Co(bpy) ₃]Cl ₃ in water	31
Cu ²⁺ /Cu(s)	0.73	p	1 M CuSO ₄ in water	33
Zn ²⁺ /Zn(s)	0.64	p	1 M ZnSO ₄ in water	33
NiO/NiOOH	1.05/2.83	p	1 M NiSO ₄ in water	33*

*According to the unified concept in this perspective, the p-type electrolyte is with negative

corrected thermopower, the n-type electrolyte is with positive corrected thermopower.

*1.05 is for range $\Delta T = 5\text{--}30\text{ }^\circ\text{C}$ and 2.83 for the range of $\Delta T = 30\text{--}60\text{ }^\circ\text{C}$

In addition to the thermopower, the figure of merit ZT is another important parameter for evaluating the energy performance of thermoelectric systems.¹⁶

$$ZT = \alpha^2 \frac{\sigma}{\kappa} \quad (5)$$

Where σ is ionic conductivity and κ is thermal conductivity of the material. While the modified figure of merit has been introduced in some materials for TECs applications.¹⁷

$$ZT = \alpha^2 \frac{D_{lim} c z^2 F^2}{\kappa R} \quad (6)$$

Where z is the charge of the ion, c is the concentration of the redox couple, R is the gas constant, D_{lim} is the limiting diffusion coefficient. The largest power generation efficiency is determined by figure of merit under a certain temperature difference. Though the desirable ZT is more than 2 for efficient devices,¹⁸ the practical ZT value is still very low. High ZT values can be obtained from high ionic conductivity and thermopower as well as low thermal conductivity. The ordinary thermoelectric semiconductor materials are usually with high conductivity, high thermal conductivity but low thermopower, since the carrier contributes to heat transfer and conduction, increasing ZT becomes an intrinsic problem. However, for the liquid-based systems, ionic conductivity, thermal conductivity and thermopower are influenced by more factors. Therefore, more methods are available to improve ZT .

The last parameter is thermal-electrical efficiency (related to Carnot efficiency) which is named as power conversion efficiency. The efficiency is expressed as :

$$\eta = \eta_c * \eta_r = \eta_r \frac{T_H - T_L}{T_H} \quad (7)$$

$$\eta = \frac{1/4 V_{oc} I_{sc}}{A k (\Delta T / d)} \quad (8)$$

where η is thermal-electrical efficiency, η_c is Carnot efficiency, η_r is relative power

conversion efficiency which indicate the final heat conversion occupies proportion of heat from Carnot cycle, T_H and T_L are the temperatures of hot side and cold side respectively, V_{oc} is the open circuit voltage, I_{sc} is the short circuit current, A is the cross sectional area, d is the electrode separation distance.¹⁹ As the maximum mean power density is reached near half of the open circuit potential,¹³ the term $1/4V_{oc}I_{sc}$ represents the maximum power output. While the term $Ak(\Delta T/d)$ is the input thermal energy to maintain the temperature difference. However, due to the low current, the output of TECs is small. When thermal-electrical efficiency is combined with equation (3), the thermal-electrical efficiency is given as:

$$\eta = \frac{1}{\frac{4\Delta S j_{sc} RT}{nF}} \quad (9)$$

$$j_{sc} = \frac{I_{sc}}{A} \quad (10)$$

$$R_T = \frac{d}{k} \quad (11)$$

where j_{sc} is the short circuit current density, R_T is the thermal resistance of TECs. Since the heat-to-electricity efficiency is usually less than 1%, lower than the expected efficiency (2%-5%) for practical energy harvesting application.²⁰ Further efficiency improvement of TEC requires the development of electrolyte with low thermal conductivity, redox couple with high reaction entropy and electrodes with high ionic conductivity and fast kinetics.¹³

Firstly, in order to increase the Carnot efficiency, the larger difference of operating temperature is required. Hence the electrolyte system and separator need to be explored for operating with higher temperature difference. Some non-aqueous electrolytes have a higher maximum working temperature. With the low boiling point of an aqueous system, various ionic liquid-based electrolytes have been explored due to their high boiling point, high ionic conductivity and low thermal conductivity, which theoretically indicate a higher ZT at a higher temperature. What's more, the large temperature gradient can be produced by lowering the thermal conductivity, which means that higher power is available. For instance, the improved electrolyte led to 66%

increase in ionic conductivity and nearly 6% decrease in the thermal conductivity, and thus produced the highest thermocell power density (12 W m^{-2}) of TECs with a temperature difference of $90 \text{ }^\circ\text{C}$.²¹

However, the thermopower of the redox couple highly depends on the nature of the ionic liquid. It is shown that the thermopower of $0.4 \text{ M I}^-/\text{I}_3^-$ in ionic liquid (from $0.03\text{-}0.26 \text{ mV K}^{-1}$) is lower than that in aqueous (0.53 mV K^{-1}) or organic solvents (0.34 mV K^{-1}). Particularly the value increases with decreasing concentration of redox couple because more solvent ions are available to solvate the redox ions in ionic liquid with lower concentration, thereby the environment of solvation environment is accentuated.²² The relationship between thermopower and concentration of redox couple matches Sosnowska's modelling prediction very well. Moreover, as introduced by the authors, quantitative structure–property relationship (QSPR) and read-across techniques could be utilized to explore higher thermopower ionic liquids with particular structure features. For example, the ionic liquids with smaller size, symmetric and less branching of ionic ions cation and high vertical electro-binding energy of the anion are predicted to have higher thermopower.²³

Specially, the biggest challenge for utilizing ionic liquid is the high viscosity of some types of ionic liquid. Thus, organic mixed electrolyte systems have been investigated in terms of improving mass transport properties which can be indicated by the diffusion coefficient. The results have been shown as expected, the diffusion coefficients of mixed electrolyte systems (1:1 ionic liquid: PC (Propylene carbonate)) are much higher than those of pure ionic liquids. For example, it is around $7.7 \times 10^{-11} \text{ m}^2 \text{ s}^{-1}$ of $[\text{Co}(\text{bpy})_3]^{2+/3+}$ in mixed electrolyte systems ($[\text{C}_4\text{mim}][\text{NTf}_2]$ and PC) but $1.2 \times 10^{-11} \text{ m}^2 \text{ s}^{-1}$ in neat ionic liquid ($[\text{C}_4\text{mim}][\text{NTf}_2]$), leading to a higher power density of mixed electrolyte systems. The power density is 7.78 mW m^{-2} of mixed electrolyte systems and 2.04 mW m^{-2} of neat ionic liquid.²⁴

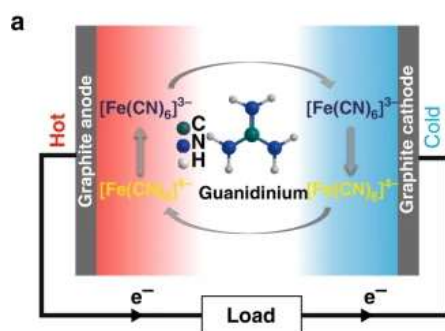


Fig. 1. Power generation of the cell using 24 M urea and 2.6 M GdmCl with cyanide electrolyte. Reprinted with permission from ref. 26. Copyright 2018 Nature.

Secondly, improving the intrinsic character is a practical way to increase the potential and current generated from the cell, which requires redox couple with high thermopower. A series of aqueous and non-aqueous redox couples have been extensively investigated. Most of the redox couples are metal ion-based couples. It is reported that $(\text{Fe}(\text{ClO}_4)_2/\text{Fe}(\text{ClO}_4)_3)$ has the highest thermopower (1.76 mV K^{-1}) among the reported $\text{Fe}^{2+}/\text{Fe}^{3+}$ salt system with different counter ions due to altered solvation shells of $\text{Fe}^{2+}/\text{Fe}^{3+}$ because of the non-covalent interactions.¹⁵ Particularly, the thermopower of aqueous ferri/ferrocyanide ($[\text{Fe}(\text{CN})_6]^{3-}/[\text{Fe}(\text{CN})_6]^{4-}$) is less concentration-dependent than other redox couples. The high thermopower of aqueous ferri/ferrocyanide ($[\text{Fe}(\text{CN})_6]^{3-}/[\text{Fe}(\text{CN})_6]^{4-}$) is attributed to the large reaction entropy.²⁵ The impressive 4.2 mV K^{-1} thermopower is achieved by enlarging the entropy change by guanidine chloride (GdmCl) and urea (Fig. 1). The higher charge of $[\text{Fe}(\text{CN})_6]^{4-}$ causes “packed” solvation shell, resulting in the stronger reaction with Gdm^+ . While urea tends to bond with $[\text{Fe}(\text{CN})_6]^{3-}$, leading to the synergistic effect of the significant entropy change.²⁶ And by utilizing the similar crystallization effect with the reactant ions, the reaction balance is changed to a preferable direction,²⁷ which brings high power density of 6.86 W m^{-2} and thermopower of 3.73 mV K^{-1} with temperature difference of $51 \text{ }^\circ\text{C}$. Besides GdmCl, a series of redox inactive ions have been added to the $[\text{Fe}(\text{CN})_6]^{3-/4-}$, $[\text{Fe}(\text{H}_2\text{O})_6]^{3+/2+}$ electrolyte to explore the non-covalent interactions, reaction

entropy change, water structure in reaction kinetics. The entropy change in $[\text{Fe}(\text{H}_2\text{O})_6]^{3+/2+}$ significantly depends on the anion structure breaker such as ClO_4^- and Cl^- while the entropy change in $[\text{Fe}(\text{CN})_6]^{3-/4-}$ relies on the cation structure making such as Li^+ . The phenomenon is due to the non-covalent interactions induced by the inert ions as supporting electrolyte, leading to the altered solvation shells. By adding the structure making or breaking ions, the negatively charged electrostatic center will attract or repel the new ions through electrostatic interaction. This leads to the rearrangement of water-CN structure. The interaction within the solvation shell of redox specie can be observed by FTIR (Fourier-transform infrared spectroscopy), where different structure making/breaking ability will result in lesser peak displacement. The higher thermopower can be obtained by adding suitable inactive ions to produce the larger entropy. However, the reactions kinetics should be carefully considered because the ions may tightly couple with the water molecules after adding structure making cation, which requires higher energy to restructure and consequently lowering the reaction kinetics.²⁸

Cobalt-based redox couple has been demonstrated to perform well in both aqueous and non-aqueous systems, which provides an optional substitute for iron based redox couple. The thermopower of cobalt-based redox couple in ionic liquid is relatively high. The highest thermopower is 2.36 mV K^{-1} using $\text{Co}^{2+/3+}(\text{py-pz})_3$ complex owing to small radius, the bi-dentate ligands, lower degree of charge delocalization and the change in electronic spin state, compared to the other complexes investigated.²⁹ The reported highest output can reach up to 880 mW m^{-2} .³⁰ While the thermopower of $\text{Co}^{2+/3+}(\text{bpy})_3$ redox couple is influenced by the solubility, supporting electrolyte, electrode surface area, diffusion rate.³⁰ However, though the thermopower of $[\text{Co}(\text{bpy})_3]^{2+/3+}$ in water (1.21 mV K^{-1}) is lower than that in organic solvents, the diffusion rate is higher than that in organic solvents, which offers faster mass transport and higher current.³¹

With the very early redox couples (such as ferric/ferrous and ferri/ferrocyanide redox couple)

widely applied, iodide/triiodide redox couple (0.97 mV K^{-1})³² and other metal based redox couples are under development. However, the reported redox couple combined with the solid metal and aqueous ion requires consumption of metal, which is not available for the continuous power generation. Burmistov's group used the traditional scheme of a thermogalvanic cell to investigate metal electrodes. The high thermopower of nickel electrode may be attributed to the nickel and hydroxides on electrode surface. The possible decay process of transformation of hydroxides of three and divalent nickel results in the 2.83 mV K^{-1} thermopower.³³ The thermopower of different redox couples is listed in Table 1 which is compared with the thermopower of thermoelectric materials in Fig. 2.⁸

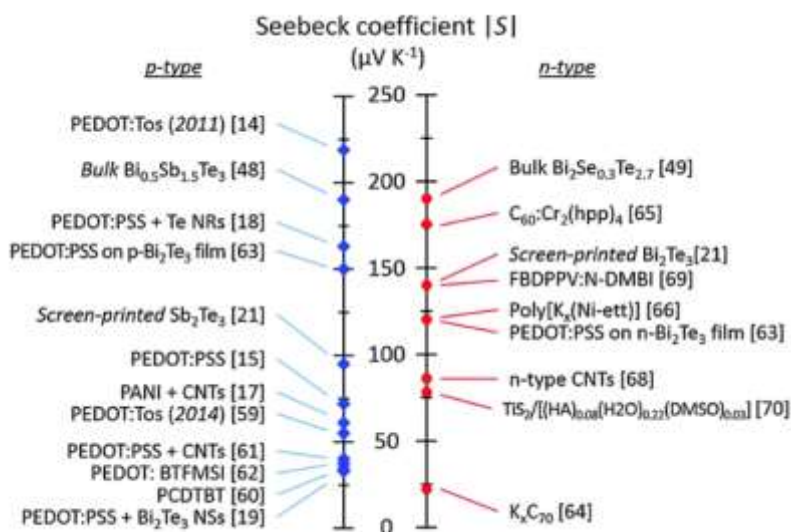


Fig. 2. The thermopower of thermoelectric materials for both p-type and n-type. Reprinted with permission from ref. 8. Copyright 2015 Royal Society of Chemistry.

Thirdly, more and more researches aim to increase the I_{SC} and lower the R_T , which in turn can boost the power output. The current density depends on the voltage according to the Butler-Volmer equation, the diffusion rate, effective surface area of the electrode, the electro-kinetic

rate constant, cell thickness and the convection.¹³ According to Nernst-Planck equation, I_{sc} consists of migration current density j_m and diffusion current density j_d . j_{sc} tends to increase with the enhanced diffusion effect because j_m and j_d are positively related to concentration gradient and diffusion rate. This was proved by Salazar's group. The kinetic and mass transfer resistance analysis of 0.4M potassium ferri/ferrocyanide demonstrates that the current density is mainly limited by the low diffusion rate at cold electrode. The greater consumption of redox couple at cold electrode results in current density reaching the limiting value.¹³ However, high diffusion rate does not always provide higher current density. Kim and co-workers³⁴ explored the diffusion and current generation in porous electrode by both quantitative description and experimental method. $Fe(ClO_4)_2/Fe(ClO_4)_3$ is utilized in their TEC. They tried to increase the current by increasing the volume of the porous electrode. However, the current density increases from 11.3 A m^{-2} with one-layer carbon fiber lamination to 16.4 A m^{-2} with four-layer carbon fiber lamination. The average current density per layer even decreases from 11.3 A m^{-2} with one-layer carbon fiber lamination to 4.1 A m^{-2} with four-layer carbon fiber lamination. The decreased effectiveness can be explained that the ion concentration decreases with ion diffusing through the electrode. The generated current becomes smaller due to the consumption of ions along the way into the electrode layer. It means that the ion diffusion hampers the high current density inside the porous electrode.³⁴

The j_{sc} can also be improved by increasing the effective area. The carbon-based electrode shows a promising potential to increase the j_{sc} and efficiency because of its large surface area. Carbon-based electrodes are possibly alternative to Pt electrode for their low cost. The highest energy relative power conversion efficiency η_r reported is up to 3.95% , the maximum power density is 6.6 W m^{-2} when applying high surface area carbon-nanotube aerogel electrode with a temperature difference of $51 \text{ }^\circ\text{C}$.³⁵ As excellent nanometer thermoelectric materials, carbon-based materials including MWNT,¹⁹ carbon single-walled nanotube (SWNT)/reduced graphene

oxide (rGO)³⁶ show potential to be applied to TECs with high energy efficiency. The reason is explained by Hu et al.¹⁹ that the large j_{sc} generated by MWNT is caused by the large number of redox reaction sites established by the large surface of electrode. Consequently, the electron transfer at the electrode-electrolyte surface is enhanced by the fast kinetics.

Finally, the structural design of the thermoelectric devices also significantly influences the energy efficiency. Teflon cell, Mark II TEC, coin-type TEC and Teflon flow cell are introduced and examined with MWNT electrode. The mass transfer is strengthened by decreasing the distance between electrodes. The relative power conversion efficiency η_r is up to 1.4%, which is higher than other structures.¹⁹

The structure of adjustable series-connected TEC arrays shows a promising potential in the wearable devices. Due to the low voltage of single TEC, adjustable series-connected TEC arrays may expand the working voltage window. A basic simple TEC device is established based on p-type electrolyte and n-type electrolyte corresponding to the n-type and p-type elements of a conventional thermoelectric generator. p-type electrolyte ($[\text{Fe}(\text{CN})_6]^{3-}/[\text{Fe}(\text{CN})_6]^{4-}$, -1.42 mV K^{-1}) and n-type electrolyte ($\text{Fe}(\text{ClO}_4)_2/\text{Fe}(\text{ClO}_4)_3$, 1.76 mV K^{-1}) use redox couple of opposite thermopower, leading to the same current direction in possible series path¹⁵. However, the $\text{Fe}(\text{ClO}_4)_2/\text{Fe}(\text{ClO}_4)_3$ electrolyte is actually p-type electrolyte and the $[\text{Fe}(\text{CN})_6]^{3-}/[\text{Fe}(\text{CN})_6]^{4-}$ electrolyte is actually n-type electrolyte according to our definition. The TEC arrays with solidified electrolyte can be explored in such long cycle time applications such as wearable electronic system because of the outstanding mechanical properties without leakage problem. The solid state of semisolid state electrolyte enables the integration of TECs in large scale. Yang et al.³⁷ assembled integrated gel-based flexible thermocell. The gel electrolyte contains Poly(vinyl alcohol) (PVA) and redox couples ($\text{FeCl}_2/\text{FeCl}_3$ and $\text{K}_4\text{Fe}(\text{CN})_6/\text{K}_3\text{Fe}(\text{CN})_6$). The thermopower of PFC gels ($\text{FeCl}_2/\text{FeCl}_3$) is 1.02 mV K^{-1} while that of PPF gels ($\text{K}_4\text{Fe}(\text{CN})_6/\text{K}_3\text{Fe}(\text{CN})_6$) side is -1.21 mV K^{-1} . But the mean thermopower is 0.6 mV K^{-1} which

is lower than those of PFC and PPF because of the significant thermal contact resistance. The generated voltage varies linearly with the temperature. The device containing 59 PFC and PPF can deliver a voltage of 0.85 V and a power output of 0.3 μW with a temperature difference of 12 $^{\circ}\text{C}$.³⁷ Although it provides high voltage, maximum power output is still low, which is possibly owing to the poor mass transportation of solidified electrolyte.

However, with researches focusing on the efficiency, the researches in optimization of power output of TEC are limited. The reported highest power is 12 W m^{-2} by improving electrolyte (0.9 M $\text{K}_3\text{Fe}(\text{CN})_6/(\text{NH}_4)_4\text{Fe}(\text{CN})_6$), electrolyte-filled thermal separators (sponge thermal separator), carbon electrode materials (activated carbon cloth).²¹

2.2 Thermally regenerative electrochemical cycles (TRECs)

In order to create the temperature gradient to utilize Seebeck effect, the TEC is designed to separate the hot and cold electrode, which produces a distance between two electrodes. Therefore, the relatively high ohmic resistance caused by the significant distance between the two electrodes leads to a low energy efficiency. This ohmic loss can be reduced by narrowing the distance while setting the temperature-dependent redox couples at different time. Thermally regenerative electrochemical cycles (TRECs), convert a full electrochemical process in spatial dimension at a certain time into four steps including charging and discharging processes in sequential.

TREC is designed to possess two electrodes with opposite thermopower. According to recent reports, the thermopower of cathode and anode are mostly negative and positive respectively. As above mentioned, the thermopower of the cell is determined by the total entropy change in the full cell reaction. If α_{cell} is negative, the cycle is correspondingly cooling - discharging - heating - charging while if the α_{cell} is positive, the process turns to be heating - discharging - cooling - charging.

A dimensionless parameter y has been introduced to adjust to TRECs electrode material.

Compared with ZT, the electric conductivity is changed to specific charge capacity while the thermal conductivity is replaced by specific heat. y is used to describe the character related to efficiency which is also similar to ZT merit of figure ($y = \alpha q_c / c_p$), where q_c is the specific charge capacity, c_p is the specific heat of an electrode. y is calculated to evaluate the efficiency. Apparently, y is increased with the higher thermopower and specific charge capacity and lower specific heat of an electrolyte ¹².

The calculation of conversion efficiency can be defined as the net work (W) divided by the input heat (Q). For the net work, the maximum output is $\Delta T \Delta S$ minus the energy loss both at high and low temperature (mainly because of the resistance). The input heat can be divided into two steps. In the first heating step, the energy of raising temperature of system Q_{HR} is relevant to the heat recuperation efficiency. It is expressed as $Q_{HR} = (1 - \eta_{HR}) C_p \Delta T$, where η_{HR} is the efficiency of recuperation efficiency and C_p is the total heat capacity of the whole cell. The second heating charging process, the total input energy at high temperature is Q_H ($Q_H = T_H \Delta S$). So the efficiency of heat to electricity is given below:^{44,45}

$$\eta = \frac{\Delta T \Delta S - W_{loss}}{T_H \Delta S + (1 - \eta_{HR}) C_p \Delta T} \quad (12)$$

While:

$$\Delta T \Delta S = \alpha_{cell} Q_c \Delta T \quad (13)$$

$$W_{loss} = I(R_H + R_L) \quad (14)$$

$$Y = \frac{\alpha_{cell} Q_c}{C_p} \quad (15)$$

$$\eta_c = \frac{T_H - T_L}{T_H} \quad (16)$$

Where Q_c is the charge capacity of the cell, C_p is the total heat capacity of the cell, α_{cell} is the thermopower of the whole cell, R_H and R_L are internal resistance at high and low temperature respectively, I is the current used in charging and discharging processes. The efficiency related to Carnot efficiency is shown below:

$$\eta = \eta_c \frac{1 - I(R_H + R_L) / |\alpha_{cell}| \Delta T}{1 + \eta_c (1 - \eta_{HR}) / |Y|} \quad (17)$$

$$\eta_r = \frac{1 - I(R_H + R_L) / |\alpha_{cell}| \Delta T}{1 + \eta_c (1 - \eta_{HR}) / |Y|} \quad (18)$$

Besides the efficiency, the maximum power output (P_{max}) is obtained when the load resistance is equal to the resistance of the cell.

$$I = \frac{\alpha_{cell} \Delta T}{2(R_H + R_L)} \quad (19)$$

$$P_{max} = \frac{(\alpha_{cell} \Delta T)^2}{8(R_H + R_L)} \quad (20)$$

However, the efficiency formula does not take consideration of the effect of energy loss W_{loss} on the heat exchange. The modified equation is given by Chen:³⁹

$$\eta = \frac{\Delta T \Delta S - W_{loss}}{T_H \Delta S + (1 - \eta_{HR}) C_p \Delta T - W_{loss} / 2} \quad (21)$$

Fig. 3 shows the development and performance of different thermoelectric technologies including their power densities and relative efficiency relative to Carnot. The power density of TREC is approximately ranging from 1 to 10 W m⁻²,⁴⁰ however, actually this value should be lower than 1 W m⁻² based on our calculations. The point is the unit conversion of non-metal solid electrode TREC from W g⁻¹ to W m⁻². The typical power density cases are given as approximately 0.178 W m⁻²,³⁸ 0.015 W m⁻²,⁴¹ 0.015 W m⁻²,⁴² and 0.332 W m⁻².⁴³ The power density is hindered by the resistance of the cell including the resistance of the solution and the cell structure, more importantly, caused by low mass transfer of ions. In comparison with the theoretical voltage value, the potential of the whole cell is relatively low with the small output current. This overpotential arises from the mass transfer problem. This still requires further research to enhance the power density.

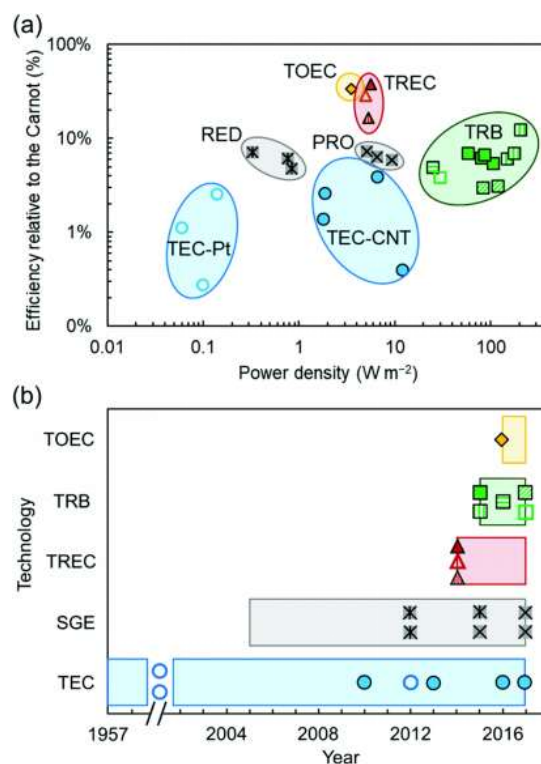


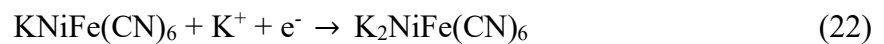
Fig. 3. Comparison of low-grade thermal energy conversion approaches, (a) The power density and efficiency relative to the Carnot (b) The research time of different approaches, TEC with platinum (TEC-Pt) or with carbon nanotube electrodes (TEC-CNT); SGE (salinity gradient energy) systems including RED (reverse electro-dialysis) and PRO (pressure retarded osmosis); TREC; TRB and TOEC. Reprinted with permission from ref. 40. Copyright 2018 Royal Society of Chemistry.

TREC was first reported in the 19th century. Nowadays researches of TREC have turned from harvesting high-temperature heat (such as from fuel cell⁴⁸⁻⁵⁰) to harvesting low grade waste heat. The entropy change during charging-discharging cycle is also applied in the desalination field to explore solar, geothermal and wind energy.⁵¹⁻⁵³ Combining the deintercalation process of sodium ion and potassium ion battery, with applying Prussian blue analog (PBA), TREC shows advantages of good stability and long cycle life of this reversible process.

2.2.1 Non-metal solid electrode.

Typical cases are TRECs based on PBA.³⁸ A copper hexacyanoferrate (CuHCF) cathode and Cu/Cu²⁺ anode with ion-selective membrane and aqueous copper nitrate (anolyte) and a sodium nitrate (catholyte) electrolyte form the main parts of this cell. The thermopower α_{cell} of whole system is up to -1.20 mV K⁻¹, while -0.36 mV K⁻¹ of cathode and 0.83 mV K⁻¹ of anode respectively. When discharging at low temperature 10 °C (charging temperature at 60 °C), sodium ions insert into the cathode material and copper dissolves into the anolyte. The maximum thermal conversion efficiency is up to 5.7% with the thermal-electrical efficiency relative to Carnot efficiency η_r of 38%.

One issue in this TREC is the anion exchange membrane, which is designed to prevent the side reaction between Cu and CuHCF. It might lose perm-selectivity at high temperature after cycles. A membrane-free PBA based TREC has been developed by switching the redox couple. Using NiHCF cathode (-0.62 mV K⁻¹), Ag/AgCl anode (0.12 mV K⁻¹), and KCl electrolyte, this TREC reaches maximum thermal efficiency of 3.5% with the thermal-electrical efficiency relative to Carnot efficiency η_r of 29% between 15 °C and 55 °C. Reactions are shown below:⁴¹



A similar cobalt hexacyanoferrate (CoHCF)-based system was also investigated, using the same Ag/AgCl anode. The thermopower (0.89 mV K⁻¹) and energy conversion efficiency (1.91%) of CoHCF with helical carbon nanotubes (HCNTs) appeared to be higher than those of the pure CoHCF (0.69 mV K⁻¹, 0.77%). This indicates that complexed PBA with carbon material may promote the efficiency.⁴⁶

Most of researches referred above focus on the materials with negative thermopower. Spinel lithium manganese oxide (LMO) is introduced as a possible material with 0.48 mV K⁻¹ thermopower in organic electrolyte with its fast kinetics during intercalation/deintercalation

process. An aqueous electrochemical system is assembled with LMO (0.62 mV K^{-1}) cathode and CuHCF anode.⁴⁷ The whole cell thermopower is 1.061 mV K^{-1} , which determines the generated voltage of high temperature higher than that of low temperature. It results in the cooling-discharging-heating-charging cycle, which is more of thermally regenerative electrochemical refrigerator. The efficiency reaches 1.8% with 10-40 °C temperature scale. The LMO cathode and CuHCF anode are based on the lithium ion and potassium ion intercalation/deintercalation reaction respectively.⁴⁷

The TREC performance may be limited for harvesting higher temperature due to the degradation and side reactions. High temperature causes capacity decay problem. The authors also investigated the effects of the electrolyte component and states of charge (SOC) on thermopower. The entropy change varies from the SOC, which means temperature response closely corresponding to SOC. Another heat harvesting system based on organic LiCoO_2/Li cells is constructed as stacks. The efficiency of dual-temperature dual-stack system based on homemade LiCoO_2/Li coin cells is 0.22%. Though the efficiency is not high, the system is attractive for self-powered sensor networks.⁴⁸

The TRECs referred above need additional charging process as the deintercalation cannot happen spontaneously after metal ions insertion. Therefore, an additional potential is needed to initiate the status. A charging free system has been reported by using increasing temperature pour cell and initiate the state. This charging free electrochemical system consists of inexpensive ferri/ferrocyanide redox couple and solid Prussian blue particles as active materials at both electrodes. The voltages of two electrodes change respectively due to their different thermopower. The two voltages start at different initial potential and cross over at a point, which indicates the self - conversion of cathode and anode induced by temperature. When this TREC works at 20 °C and 60 °C, the heat to electricity conversion efficiency is 2.0%.⁴²

Actually, the complete cell requires the two electrodes to have a positive thermopower and

negative thermopower respectively. Usually, the thermopower can be enlarged by more negative thermopower of cathode and more positive thermopower of anode, which ensure the negative α_{cell} (the cycle is correspondingly cooling - discharging - heating - charging) to harvest heat.

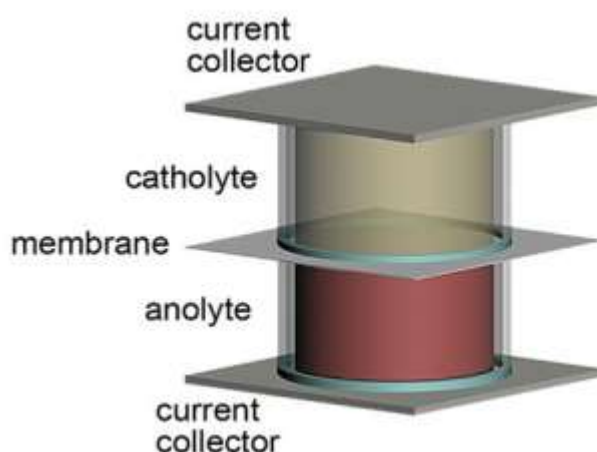


Fig. 4. Schematic of the battery design, 0.5 M $\text{K}_3\text{Fe}(\text{CN})_6$ /0.1 M $\text{K}_4\text{Fe}(\text{CN})_6$ (catholyte) versus 0.1 M I_2 /2 M KI (anolyte). Reprinted with permission from ref. 43. Copyright 2019 Royal Society of Chemistry.

Apart from the traditional method for heat utilization, a novel system (Fig. 4) for simultaneous energy conversion and storage via solar driven regenerative electrochemical cycles is designed by Ding et al.⁴³ The anode functions as both bifunctional current collector and solar absorber under solar irradiation. $\text{K}_4\text{Fe}(\text{CN})_6/\text{K}_3\text{Fe}(\text{CN})_6$ and KI/KI_3 are selected by evaluating the limiting diffusion current and reaction rate constant, which show fast kinetics to overcome the sluggish mass transport and reaction activation. The catholyte ($\text{K}_4\text{Fe}(\text{CN})_6/\text{K}_3\text{Fe}(\text{CN})_6$, negative thermopower) and anolyte (KI/KI_3 , positive thermopower) are separated by a cation-exchange membrane, leading to the whole thermopower of -1.8 mV K^{-1} . Moreover, the carbon felt wrapped by reduced graphene oxide (rGO) acts as a solar absorber and a current collector, which greatly

boosts the temperature. A good efficiency of 1.23% is achieved with a small temperature difference of 35 °C.⁴³

As the equilibrium potential, reaction kinetics and the mass transport properties are temperature-dependent, the activation, ohmic loss, concentration loss and overpotential are affected by temperature. In fact, all the three overpotentials decreases with increasing temperature. The activation overpotential loss decreases with increasing temperature due to reduced energy barrier decreases at a higher temperature. The concentration overpotential loss also decreases with increasing temperature as the viscosity of the liquid decreases with increasing temperature, leading to favorable mass transport. In addition, the ohmic loss decreases with increasing temperature due to higher ionic conductivity of the electrolyte at a higher temperature. Thus, the performance of the TRECs can be significantly improved by increasing the temperature. However, in order to reduce ohmic and concentration loss, large current density operation should be avoided. At a high current density, concentration loss can be a limiting factor especially when the system is working at a limiting current density. In addition, the ohmic loss increases almost linearly with increasing current density. Obviously, the effective power output is limited by the current density.

Based on the experimental work, the performance characteristics of TRECs are also analyzed by modelling.^{46, 58-60} Finite time analysis is utilized to study the impacts of various operating and material parameters on performance of TRECs, giving the criterion for optimizing the performance.⁵⁰ The authors suggest the material with larger isothermal coefficients, specific charge/discharge capacities, appropriate internal resistance and lower heats is appealing. Since the regenerative efficiency does not influence the maximum power output, it means that the regenerative loss $(1 - \eta_{HR})C_p\Delta T$ referred as Q_{HR} above does not affect the power output. This is also proved by Wong et al.⁴⁹ that regenerative loss does not influence the corresponding $P_{max} = m\alpha^2\Delta T/8R$ is the number of cell charged simultaneously, where R is the resistance

in both series connection and parallel connection. However, the regenerative efficiency does have significant impact on the efficiency. The efficiency equation depicted by Wong reveals that the efficiency increases with decreasing regenerative losses. As the power output decreases with the efficiency increase when $\eta \geq \eta_p$, the objective function ηP is given to determine the operation region of current. The optimal range of the electric current should be $I_{\eta P} \leq I \leq I_p$, so $P_{\eta P} \leq P \leq P_{max}$, $\eta_p \leq \eta \leq \eta_{\eta P}$, where the subscripts ηP is the maximum efficiency-power product, P is maximum power, max is maximum.⁴⁹

2.2.2 Redox flow batteries (RFBs)

At present, redox flow batteries (RFBs) have been applied in energy storage systems. Due to the ability to storage large-scale energy, and long cycle lifetime,⁵² some researchers investigate the all-vanadium redox flow battery (VRFB) to explore the feasibility of capturing low grade heat. The principle is based on the reversible reaction of V (II) / V (III) in the negative electrolyte and V (IV)/ V (V) in the positive electrolyte. As shown in Fig. 5, V (II) is oxidized to V (III) at the negative reservoir while V (V) is reduced to V (IV) during discharge (reverse reaction of equation 23-24). Protons move from negative to cathode through the proton Nafion membrane to maintain electrical neutrality. The electrolyte continuously flows between the reservoirs and the electrode, bring ions to the electrode surface where electrochemical reaction takes place.⁵³ Owing to the different temperature responses of negative electrolyte and positive electrolyte, general TRECs can be introduced into RFBs. The created thermodynamic cycle of TREC-VRFB system is displayed in Fig. 6.

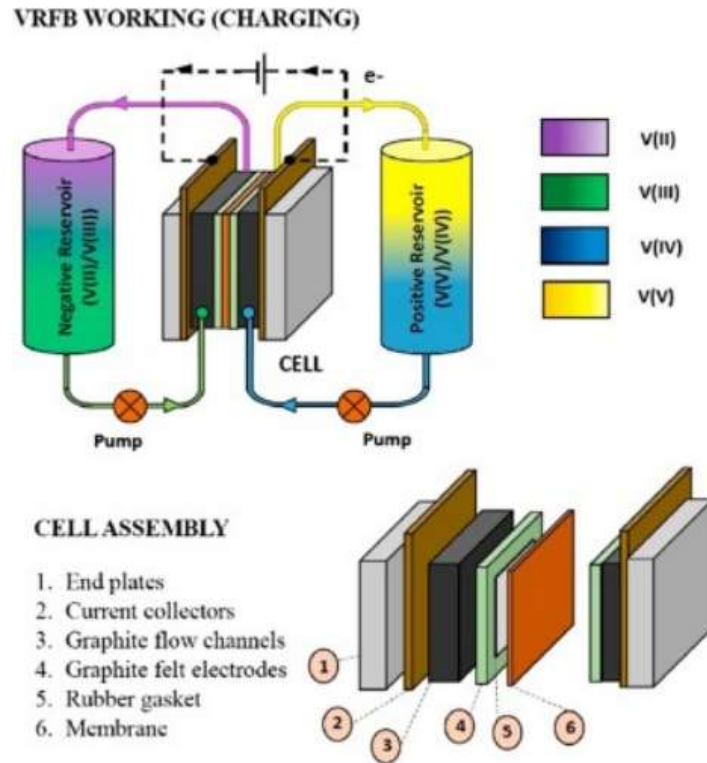


Fig. 5. The structure of VRFB. Reprinted with permission from ref. 53. Copyright 2019 Elsevier.

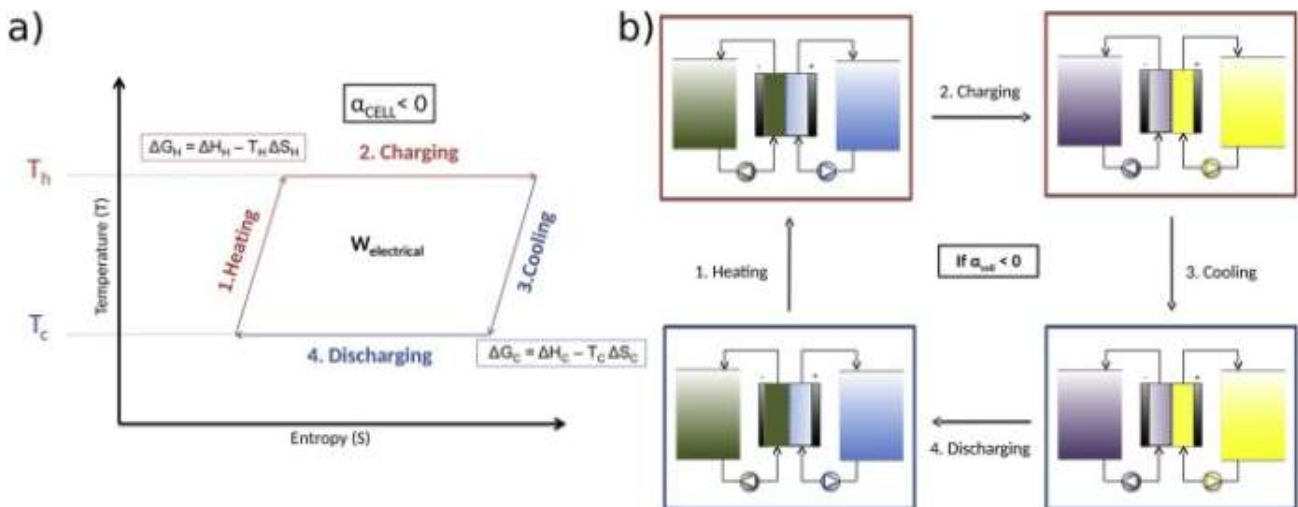


Fig. 6. The principle for harvesting heat of VRFB, a) The temperature-entropy plot for a TREC when thermopower is negative b) The thermodynamic cycle of TREC-VRFB system.

Reprinted with permission from ref. 54. Copyright 2018 Elsevier.



Reynard's group reported the thermopower of whole cell (TREC-VRFB) in commercial

electrolyte is around -1.16 mV K^{-1} while it is -0.80 mV K^{-1} in the mixed-acid electrolyte which is dominated by the negative electrolyte. The energy density is increased by 1.3 Wh L^{-1} and 0.8 Wh K^{-1} respectively.⁵⁴ This is appealing for heat harvesting and electricity generation in photovoltaic farm.⁵⁵ However, the available temperature range is limited by the instable voltage (V).⁵⁶ The operating temperature is strictly limited between $10\text{-}40 \text{ }^\circ\text{C}$ to avoid precipitation.⁵⁷ Also, the complete VRFB system is integrated by electrolyte container, electrode, pipe, pump and heat exchanger, leading to the large weight and volume and further low energy density.

Most of the existing studies on RFBs focus on the battery performance without detailed discussions on the energy efficiency of the whole system. The energy efficiency of the RFB system should fully consider the additional pumping power and other losses. The efficiency can be determined using equation below:

$$\eta = \frac{I(\Delta V - I(R_H + R_L)) - I^2 R_{Lead} - P_{aux}}{IT_H \Delta \alpha + Q_{loss} + (1 - \varepsilon_{HX}) \dot{m} C_p \Delta T} \quad (26)$$

where R_{Lead} is the resistance of the electrical leads, $\Delta \alpha$ is the difference of thermopowers, P_{aux} is auxiliary power input (it is mainly pumping power in this system), $(1 - \varepsilon_{HX}) \dot{m} C_p \Delta T$ is the heat leaks from the mass transport of reactants, ε_{HX} is the effectiveness of the recuperative heat exchanger and \dot{m} is the mass flow rates of the fluids respectively.⁵⁸

Similarly, a continuous electrochemical heat engine⁵⁸ also exploits the flow electrolyte with aqueous $\text{V}^{2+}/3+$ (1.7 mV K^{-1}) and $\text{Fe}(\text{CN})_6^{3-}/4-$ (-1.4 mV K^{-1}) to create an overall 3 mV K^{-1} of the cell. At the maximum power density of $110 \text{ } \mu\text{W cm}^{-2}$ equivalent to 1.1 W m^{-2} , the corresponding η_r and η_c are 0.15 and 12.4%, respectively. The authors believe that by using a variety of redox couples, the maximum power increases with the electrode reaction rate constant k_0 till k_0 is 0.05 cm s^{-1} . The power output is only a function of thermopower α at a high k_0 , suggesting the change in polarization and rate controlling steps. Under this circumstance, the ohmic resistance and mass transport loss are larger than activation polarization.

In other words, the ohmic and mass transport loss limit the achievable maximum power density. Changing the fluid flow patterns (improving mass transport) and increasing redox couple concentrations (improving reaction rate) both contribute to higher power density. A higher power density of 200 W m^{-2} with 15 M concentrated slurries is theoretically predicted. This high power density could be achievable for redox couples with high solubility. However, the solubility of most redox couples is insufficient.

It should be noted that in the current literature, both Wh L^{-1} and W m^{-2} are used to measure the performance of the thermoelectric cell. Wh L^{-1} is energy density. It is obtained by running a system for a certain time under a certain power condition, then divided the electrolyte volume. It evaluates the efficiency of the system. For comparison, W m^{-2} is power density, which is based on the membrane area. Comparing power densities of different systems not only gives the power generation ability, but also, is helpful to analyze the utilization and performance of membrane.

2.2.3 Thermal regenerative ammonia-based batteries (TRABs)

Since thermally regenerative acetonitrile-based all-copper redox flow battery reported before,⁵⁹ a new thermal regenerative ammonia-based batteries (TRABs) is reported to utilize low grade heat for electricity generation. Cu^{2+}/Cu cathode and $\text{Cu-NH}_3/\text{Cu}(\text{NH}_3)_4^{2+}$ are applied to this system. The electricity is generated by the formation of metal ammine complexes. While the solid copper electrodes alternative serves as anodes or cathodes in TRABs, NH_3 is separated and transferred by traditional heat-based separation technology. The theoretical voltage is up to 0.344 V. The cycle is shown in Fig. 7.⁶⁰

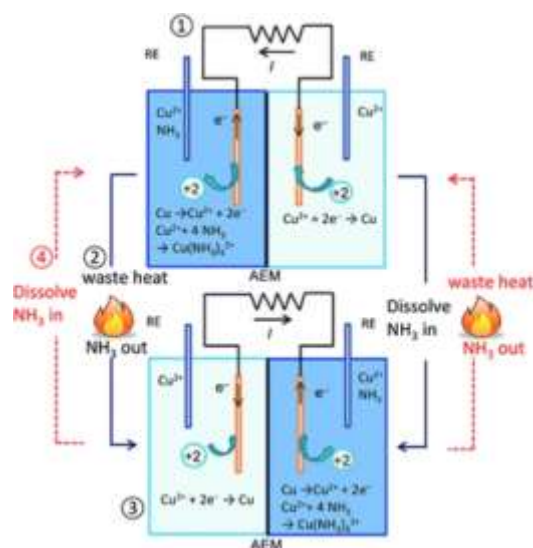


Fig. 7. The closed-cycle system for TRAB. Reprinted with permission from ref. 60. Copyright 2015 Royal Society of Chemistry.

As referred above, the solvation limitation which restricts the power density is solved by introducing high solvation NH_3 . The power output of TRABs is much larger than the highest power output of TECs (12 W m^{-2}) and RFBs (1.1 W m^{-2}), which shows great advantage for practical application. The reported power output of Cu-TRAB is 60 W m^{-2} ,^{47,67} however, the value varies from 47 to 136 W m^{-2} . With the low resistance BTMA PPO anion exchange membrane, the power output is increased to 106 W m^{-2} while the efficiency is increased to 0.97%.⁶¹ Furthermore, the ethylenediamine shows a better performance than ammonia as a ligand. The power output of ethylenediamine-based battery (TRENb) is 85 W m^{-2} with 2 M ethylenediamine and 119 W m^{-2} with 3 M ethylenediamine. However, the energy requirement of separation process of ethylenediamine is 2.5 times more than that of ammonia, which causes lower thermal-electric efficiency (0.52%). A higher thermal-electric efficiency can be obtained by examining alternative separation methods.⁶² The comparison of parameters in various system is listed in Table 2.

Table 2

The comparison of parameters in various system.

System	Power output (W m ⁻²)	η (%)	η_r (%)	Temperature (condenser- reboiler/ °C)	Reference
Cu-TRAB	60	0.86	6.2	-	60
BTMA-TRAB	106	0.97	7.0	43.3-70.4	61
TRENB	119	0.52	3.1	-	62
Ag-TRAB	23	0.41	3.8	43-60	63
Cu-TRAFB	45	0.70	5.0	43.3-71	78
Cu/Zn-TRAB	118	0.95	10.7	43-70.9	66
Cu/Zn-TRAFB	280	0.34	2.7	43-70.9	9

With the development of TRABs, the researchers focus on improving the performance. The main aspects are given below.

- 1) The poor long cycle lifetime stability. The poor reversibility is derived from the unbalanced electron exchange of anode and cathode, which means the metal is consumed in continuous cycles (less than 10 cycles). The anode coulombic efficiency (ACE) is approximately 37% while the cathode coulombic efficiency (CEE) is around 100%, resulting in the relatively low discharge energy efficiency (44%). This indicates a large portion of copper dissolved in the anode electrolyte but does not take part in the electrode reaction. This is based on the side reaction of dissolved oxygen and the formation of Cu(OH)₂, and further proved by adding acid and removing dissolved oxygen to improve the battery performance.⁶⁰ Replacing the ammonia ligand with ethylenediamine raises the ACE to 77%.⁶² Moreover, a high ACE of almost 100% is obtained by using silver

salt.⁶³ The promising value represents excellent reversibility, proved by over a hundred charge/discharge cycles of producing a stable power. Due to the high cost of silver, the metal electrode is substituted with carbon-silver electrodes.

- 2) The resistance problem. The whole resistance consists of the Ohmic resistance and the activation resistance. Both Ohmic resistance and activation resistance can be determined by electrochemical impedance spectroscopy (EIS) test. Ohmic resistance is battery internal resistance caused by the electrolyte conductivity and diffusion rate. Additionally, the reaction resistance is related to the electrode dynamics. For example, the charge-transfer resistance can judge the difficulty of the reaction kinetics: the smaller charge-transfer resistance means better reversibility of the electrode. The better reversibility of Ag compared with Cu is because of the low reaction resistance (0.08Ω).⁶³ In order to solve the resistance problem, a compact design is required to stack the electrodes and membrane together. Adding NH_4NO_3 as supporting electrolyte also enhances the electrolyte conductivity and reduces the resistance without bringing other ions and pollution. But dense NH_4NO_3 might increase the viscosity, which increases the transport resistance of copper ions, leading to high reaction resistance and energy loss. The peak power density is obtained at 3 M NH_4NO_3 concentration in the range of 1-5 M, suggesting the existence of an optimal concentration.⁶⁴
- 3) The concentration optimization of Cu^{2+} and NH_3 . The cycle stability is ensured by the consistence of cathodic Cu^{2+} concentration and the anodic $\text{Cu}(\text{NH}_3)_4^{2+}$ concentration in every cycle. Owing to the copper corrosion during discharging, the cathodic Cu^{2+} concentration is greater than the anodic $\text{Cu}(\text{NH}_3)_4^{2+}$ concentration. Therefore decreasing the initial anodic $\text{Cu}(\text{NH}_3)_4^{2+}$ concentration is necessary to avoid cyclical concentration change. Also, appropriately increasing Cu^{2+} and NH_3 concentration could improve the battery performance, because Cu^{2+} concentration determines the limiting current density

which shows mass transport ability, while NH_3 concentration has a vital effect on the power output and overpotential.⁶⁴ The power output increases from 53 W m^{-2} with 1 M NH_3 to 136 W m^{-2} with 3 M NH_3 .⁶⁰

- 4) The temperature effects. Compared with 95 W m^{-2} at $23 \text{ }^\circ\text{C}$, the maximum power density linearly increases to 236 W m^{-2} at $72 \text{ }^\circ\text{C}$. The high relative efficiency η_r (13%) is obtained with the total efficiency η of 0.5%. An improved reaction kinetics at higher temperature attested by the reduced overpotential, results in the enhancement in power production. However, the high temperature causes the loss of membrane selectivity and further brings about the ammonia crossover problem, which leading to a decrease in power density and coulombic efficiency.⁶⁵
- 5) Effect of flow rate. The use of flowing electrolyte is a practical method to strengthen mass transport. The power density of Cu/Zn-TRAFB (280 W m^{-2}) is twice more than the power density of Cu/Zn-TRAB (118 W m^{-2}).^{9,66} The power output increases with the flow rate when the flow rate is below 8 mL min^{-1} , otherwise the reaction is controlled by the kinetic rate under sufficient mass transfer.⁹
- 6) Scalability of system. The flexibility of compiling battery system in series or parallel can meet the actual demands for voltage and current.^{9,60}

2.2.4 Electrical double-layer-based cycle

The thermal induced entropy change is utilized to harvest energy by constructing electrical double-layer capacitors. One method is to make use of thermal membrane potential of ion exchange membrane to extract energy from small thermal difference,⁶⁷ or harvesting the mixing free energy of solutions of different concentrations. In particular, the electrostatic potential increases with the temperature, which enhances the ion capturing ability.^{68,69} As shown in Fig. 8, the voltage changes from 2.50 to 2.536 V at $65 \text{ }^\circ\text{C}$ temperature, the calculated thermopower of

the capacitor is 0.6 mV K^{-1} and the theoretically predicted efficiency is 5%.⁶⁸ However, both two methods are confronted with the decay problem. Thus, the power generation is not continuous, the operation process is within a certain time scale.

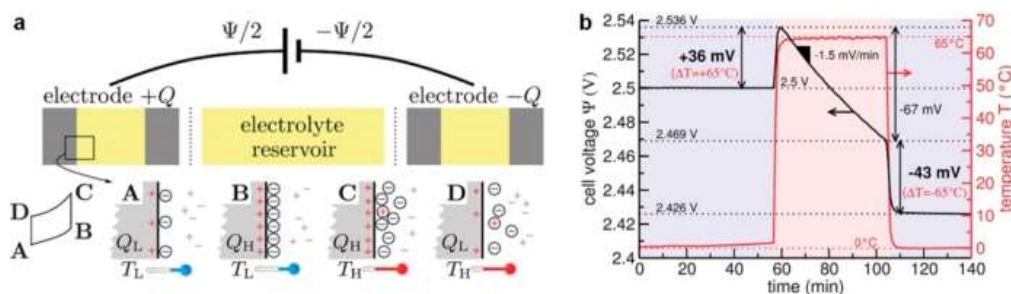


Fig. 8. (a) A supercapacitor model with two parallel plates. (b) The open-circuit potential change when cycling the fully charged cell between 0 and 65 °C. Reprinted with permission from ref. 68. Copyright 2015 Royal Society of Chemistry.

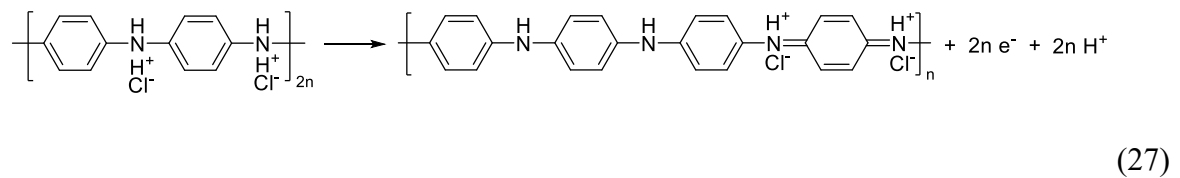
2.2.5 Direct thermal charging cell (DTCC)

Direct thermal charging cell⁶⁹ for converting low-grade heat to electricity was invented recently. In particular, this kind of isothermal heating operation does not require external charging and building thermal gradient. DTCC can be self-regenerated after discharging. While the thermopower is quite high up to 5 mV K^{-1} , the thermoelectric conversion efficiency reaches 3.52% at 90 °C with 19.7% of Carnot efficiency. Compared with the other thermal cycles and thermal conversion devices, the thermopower and efficiency are still high. However, the degradation problem of cathode limits the application which requires a long-term cycling.

DTCC consists of asymmetric electrodes (capacitor-type cathode of GO/PtNPs and a battery-type anode of anode of PANI) and aqueous electrolyte containing $\text{Fe}^{2+}/\text{Fe}^{3+}$. DTCC generates the voltage by the temperature induced pseudocapacitive GO and temperature dependent electron carriers (redox couple). The relevant electrical double layer-based cycle has been reported to thermal induced ionic entropy change which results in thermopower of 0.6 mV K^{-1} of the double

layer capacitance. The voltage change is 0.036 V of the temperature change from 0 to 65 °C. This illustrates existence of temperature-dependent capacitive effect.

At first, DTCC is heated at open circuit. Due to the pseudocapacitive effect, oxygen functional groups absorb protons and react at the electrode-electrolyte interface. Due to the positive thermopower of the $\text{Fe}^{2+}/\text{Fe}^{3+}$ redox couple, the reduction reaction happens with the increase in temperature. The open circuit voltage is enhanced by the two effects. Then connecting the two electrodes, PANI self-oxidizes while electrons transfer to cathode to attribute to reduction of Fe^{3+} . At the last regeneration stage, oxidized PANI reacts with Fe^{2+} and reverts to the initial stage. The reaction is given below:



DTCC exhibits excellent efficiency and power density. What's more, potential applications including a wide operation window, and low-cost cell stacks are under exploration. But it still remains an ongoing challenge of cyclability which requires further research like changing the cathode materials or redox couple to tackle the degradation problem. Furthermore, the mechanisms of reactions of temperature induced pseudocapacitive effect together with the PANI polymer catalytic activation have yet to be identified.

2.3 Thermo-osmotic energy conversion (TOEC)

Thermo-osmotic energy conversion (TOEC) is a new technology based on the hydrophobic membrane. When the temperature gradient tends to drive the vapor flux against a hydraulic pressure difference, a pressurized flow is produced to drive a turbine or other types of machines.

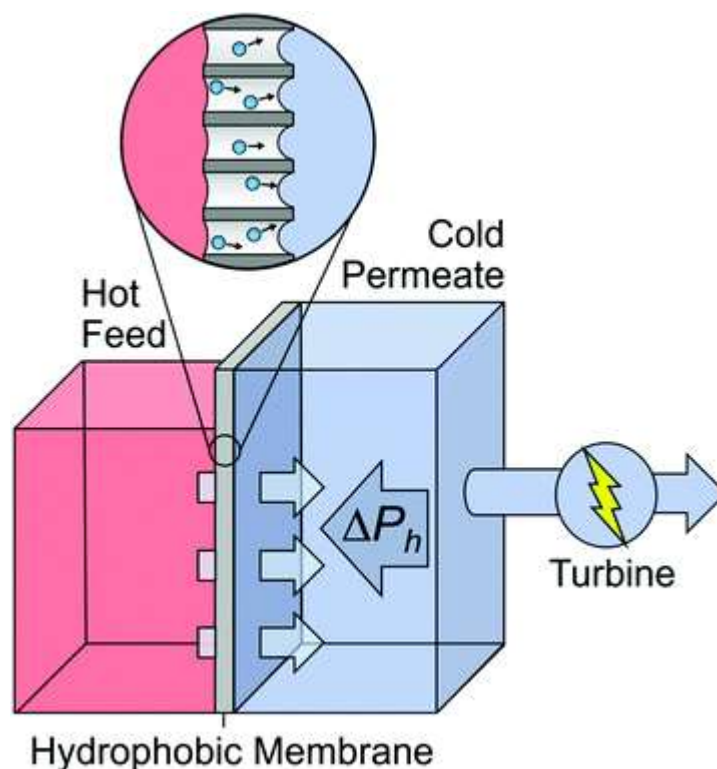


Fig. 9. Working principle of TOEC system, a, Schematic diagram of water vapour transport across a membrane, b, Hydraulic pressure that can be theoretically generated with a certain temperature difference across a membrane. Reprinted with permission from ref. 40. Copyright 2018 Royal Society of Chemistry.

As demonstrated in Fig. 9, applying a hydrophobic, nanoporous membrane between hot and cold liquid creates a gas phase, temperature-driven flux against the pressure-driven flux from the hot side to the cold side. Consequently, the volume of the cold liquid hinders the expansion and leads to the pressure to the turbine for power generation. Water is used in this system due to its high surface tension, which prevent the membrane pore from infiltration. Vapor-gap membrane is used in this system because of their relatively high thermo-osmotic fluxes and relatively low thermal conductivity of polymer membrane. Polytetrafluoroethylene (PTFE) has been first used in this system, producing $3.53 \pm 0.29 \text{ W m}^{-2}$ power density with $40 \text{ }^\circ\text{C}$ temperature difference

(20 °C-60 °C). The efficiency of optimized system with continuous closed-loop system is more than 50% of Carnot efficiency.⁷⁰

The thermal efficiency of the membrane is the amount of heat transferred by vaporization through the membrane divided by the total heat transferred. The heat loss mainly is due to the thermal conductivity of the membrane. Thermal efficiency is relevant to the thermal conductivity and thickness of membrane. In order to increase the efficiency, reducing thermal conductivity is a practical way.⁷¹ The working fluid investigated by now is water because of high surface tension and high heat of vaporization, however, mixing of fluids, such as working fluid with different absorption of CO₂ also show potential of improving the performance.^{70,73} More importantly, a higher efficiency can be obtained by increasing the pressure and a higher power can be obtained by increasing the area of the membrane theoretically. But the amelioration strategies in increasing pressure resistance and high performance structure are still under investigation.⁷¹

3. Summary and perspectives

Compared with TE, liquid-based systems show great advantages in power density, efficiency, and cost. With more and more researchers' interests and efforts in the use of liquid-based systems for recovering low-grade waste heat, the power density and efficiency have been improved significantly. However, in order to make the systems practical, the fundamental understanding and the cell design are both vital to overcome the key performance limitations.

For TECs, the key point is the redox couple and cell configuration. As most researchers focus on the efficiency improvement, the practical application of TECs is limited by the low power density (maximum 12 W m⁻²), which can be improved by changing alternative redox couple with higher thermopower, and optimizing the cell configuration.

First and foremost, a redox couple with higher thermopower requires a development in exploring the new redox couple, or maximizing the entropy change by improving electrolyte.

The detailed analyses have been discussed above. In particular, the computational modelling is under-utilised to investigate a new redox couple and additive. The simulation is supposed to theoretically explain the relationship between the thermopower and entropy change and solvent structure. Furthermore, the simulation based on the design of systems and current experimental data, provides a reasonable suggestion on the structure optimization, moreover predicts the performance of the whole system. The computational and simulation methods show a huge potential in terms of the analytical ability. Secondly, cell configuration approaches can improve the power density in certain perspectives. For example, a significant power density change is the application of electrolyte-filled thermal separators (sponge thermal separator).²¹ The increased thermal resistance attributes to larger temperature gradient inside the cell. While the proper thickness and porosity lead to decreased thermocell resistance. According to the currently achievable power density, future work of utilizing TECs possibly focus on the integrated TEC arrays for wearable devices because of the low power density requirement.

The TRECs are confronted with the same power density difficulty (below 1 W m^{-2}) which can be improved by increasing the whole thermopower of the cell, widening the temperature range, lowering the resistance. These requirements need the fundamental understanding of entropy change of material during the reaction, the advanced electrode material design with fast kinetics and higher temperature tolerance, good design of system or cell configuration and also, membrane with good selectivity and low resistance.

Firstly, the fundamental understanding of thermopower should be further studied. Since the general understanding of thermopower of redox couple is based on the solvation structure in liquid phase, the thermopower of solid phase is more complex. The influence factors including phonon entropy, configuration entropy, electron entropy. These are widely studied in the heat control system of industrial battery pack. However, we still need to trace the origin of entropy change in solid phase. As referred by Gao et al.,¹² the problems are the relation of entropy change

and properties of electrode material, the optimization in electrode material and composition. Secondly, the exploration in electrode material is needed. As the other problems such as cell configuration can be settled by technical methods, the electrode material is an urgent problem for TRECs. The material is required to make entropy contribution on the thermopower of the whole cell during the reaction, have fast kinetics and long-term stability to ensure the reaction conduction. Although the utilizing metal ion battery materials gives us a good idea, the thermopower of the whole cell is relatively low. The redox couple are possibly introduced into the TRECs. DTCC is a good example to fulfill the cycles with exploiting $\text{Fe}^{2+}/\text{Fe}^{3+}$ redox couple, but its long-term operation still needs to be further improved. What's more, the guidance on enlarging the thermopower will become clearer if more evaluation and analysis are conducted to determine the entropy contribution of solid phase and liquid phase. Thirdly, the investigation membrane is also required. As an important composition of TRECs, the membrane separates the anode and cathode. More importantly, it prevents the possible side reaction in the system. And in a specific TREC system, good selectivity and low resistance more importantly, high temperature tolerance is critical. Finally, the optimization in cell configuration is vital for real application. As for the performance of TRECs, actually, even though the low power output can be solved by connection in series or parallel, the exact problem is the small effective current density in spite of the high thermopower. In this perspective, TRECs show a certain potential in application in sensor due to the low power requirement, the smallest sensor only needs 10 mW in 10-30 cm^2 area.

Among the various types of TRECs, TRABs are the most promising practical application because of its highest power density (280 W m^{-2}) so far. The poor cycle performance can be ameliorated by replacing the metal ion. Optimizing the concentration of supporting electrolyte, ligand and metal ions, adjusting the temperature and flow rate propose a reasonable plan to maximize the power output and efficiency. Future work will probably aim to lower the cost to

achieve the perfect columbic efficiency, leading to practical large-scale power generator application.

While the major problem of TOEC is lacking of robust membrane under pressure. Some works focus on the design of the membrane to create a theoretically 88.8 W m^{-2} excitingly high power density⁷³, which shows a great potential in ecofriendly and continuous heat harvesting. However, the work in this field is limited therefore it still needs further exploration.

To sum up, the TRABs present the highest power density which followed by TECs and TOECs, which are competitive with semiconductor thermoelectric material ($\sim \text{mW cm}^{-2}$), while TOECs, TRECs and DTCC display the relatively higher efficiency. They have overlap in their functionality but have unique features and working conditions. The TRAB systems can be potentially up-scaled for large scale application for recovering industrial waste heat. The other systems such as TOECs and TECs can be applied to recover waste heat below $100 \text{ }^\circ\text{C}$, such as waste heat from air conditioners. In addition to these technologies mentioned above, there are other technologies for waste heat recovery such as organic Rankine cycle, heat recovery steam generator and heat pipe system. What's more, combination of different technologies such as triboelectric, pyroelectric, piezoelectric, thermoelectric, thermal-electrochemical systems⁷⁴ establishes a new field to boost the efficiency and power density. The related materials such as ZnO nanowire arrays, polarized poly(vinylidene fluoride) (PVDF) film-based generator, both have pyroelectric and piezoelectric properties. The assembled hybrid cell can harvest thermal, mechanical and solar energy simultaneously.⁷⁵⁻⁷⁷

Conflict of interest

The authors declare that they have no conflict of interest.

Acknowledgements

M. Ni thanks the funding support from Hong Kong Polytechnic University (P0014036) and a grant (Project Number: PolyU 152064/18E) from Research Grant Council, University Grants Committee, Hong Kong SAR.

Author Biographies

Chun Cheng is now a PhD student of Department of Building and Real Estate at The Hong Kong Polytechnic University. She was graduated from Harbin Institute of Technology (Bachelor) in 2019. Her research background is in electrochemistry and chemical engineering. Now her research focuses on the electrochemical method of heat to electricity conversion.

Yawen Dai is now a PhD student at The Hong Kong Polytechnic University, Hong Kong, China. She received her Bachelor's degree from Beijing Normal University, Beijing, China and Master's degree from The National Center for Nanoscience and Technology, Beijing, China. Her research focuses on materials and devices for energy conversion and storage, including photocatalysis, electrocatalysis, and rechargeable batteries.

Jie Yu completed her PhD program in Chemical Engineering from Nanjing Tech University, P. R. China, in 2018. She is now a postdoctoral fellow in Hong Kong Polytechnic University, Hong Kong, China. Her research interests focus on design and synthesis of perovskite oxides, metal sulfides, metal phosphides, and carbon composites and their applications in electrochemical catalytic fields.

Dr. Chang Liu is a postdoc fellow at the University of Hong Kong and received her Ph. D. also from the University of Hong Kong in 2018. Her research interests focus on ionic thermoelectric

materials and light/thermal management via hydrogel materials.

Sijia Wang is a Ph.D. student at Department of Mechanical Engineering, University of Hong Kong. She received her bachelor's degree from Beihang University in Materials Science and Engineering and master's degree from the Hong Kong University of Science and Technology. Her main research interests are functional material design and thermo-electrochemical energy conversion.

Dr. Shien Ping Feng is an Associate Professor at Department of Mechanical Engineering, University of Hong Kong. He received his BS, MS, PhD from National Tsing Hua University. He was a postdoctoral associate at MIT and was working in semiconductor industry before entering academia. His current research focuses on the development of electrochemical technology for energy harvesting and recycling. He is an elected Fellow of the IMMM and is the co-founder and founder of two start-up companies.

Prof. Meng Ni received his PhD from University of Hong Kong. Currently, he is a Professor and Associate Head at The Hong Kong Polytechnic University. His research interests include fuel cells, rechargeable batteries, and electrochemical systems for low grade heat utilization. Prof. Ni is a Senior Editor for Sustainable Energy Technologies and Assessments (Elsevier) and an Associate Editor for other two journals. He is an active reviewer for over 80 academic journals.

References

- (1) Lawrence Livermore National Laboratory. Estimated U.S. Energy Use in 2019: 100.2 Quads. 2019. <https://flowcharts.llnl.gov/commodities/energy>.
- (2) Haddad, C.; Périlhon, C.; Danlos, A.; François, M. X.; Descombes, G. Some Efficient Solutions to Recover Low and Medium Waste Heat: Competitiveness of the Thermoacoustic Technology. *Energy Procedia* **2014**, *50*, 1056–1069. <https://doi.org/10.1016/j.egypro.2014.06.125>.
- (3) Jouhara, H.; Khordehgah, N.; Almahmoud, S.; Delpech, B.; Chauhan, A.; Tassou, S. A. Waste Heat Recovery Technologies and Applications. *Therm. Sci. Eng. Prog.* **2018**, *6* (January), 268–289. <https://doi.org/10.1016/j.tsep.2018.04.017>.
- (4) Simeone, A.; Luo, Y.; Woolley, E.; Rahimifard, S.; Boër, C. A Decision Support System for Waste Heat Recovery in Manufacturing. *CIRP Ann. - Manuf. Technol.* **2016**, *65* (1), 21–24. <https://doi.org/10.1016/j.cirp.2016.04.034>.
- (5) Jin Bae, E.; Hun Kang, Y.; Jang, K. S.; Yun Cho, S. Enhancement of Thermoelectric Properties of PEDOT:PSS and Tellurium-PEDOT:PSS Hybrid Composites by Simple Chemical Treatment. *Sci. Rep.* **2016**, *6* (May 2015), 1–10. <https://doi.org/10.1038/srep18805>.
- (6) Saxena, N.; Pretzl, B.; Lamprecht, X.; Bießmann, L.; Yang, D.; Li, N.; Bilko, C.; Bernstorff, S.; Müller-Buschbaum, P. Ionic Liquids as Post-Treatment Agents for Simultaneous Improvement of Seebeck Coefficient and Electrical Conductivity in

- PEDOT:PSS Films. *ACS Appl. Mater. Interfaces* **2019**, *11* (8), 8060–8071.
<https://doi.org/10.1021/acsami.8b21709>.
- (7) Fan, Z.; Du, D.; Guan, X.; Ouyang, J. Polymer Films with Ultrahigh Thermoelectric Properties Arising from Significant Seebeck Coefficient Enhancement by Ion Accumulation on Surface. *Nano Energy* **2018**, *51* (May), 481–488.
<https://doi.org/10.1016/j.nanoen.2018.07.002>.
- (8) Bahk, J. H.; Fang, H.; Yazawa, K.; Shakouri, A. Flexible Thermoelectric Materials and Device Optimization for Wearable Energy Harvesting. *J. Mater. Chem. C* **2015**, *3* (40), 10362–10374. <https://doi.org/10.1039/c5tc01644d>.
- (9) Wang, W.; Shu, G.; Tian, H.; Huo, D.; Zhu, X. A Bimetallic Thermally-Regenerative Ammonia-Based Flow Battery for Low-Grade Waste Heat Recovery. *J. Power Sources* **2019**, *424* (December 2018), 184–192. <https://doi.org/10.1016/j.jpowsour.2019.03.086>.
- (10) Zeb, K.; Ali, S. M.; Khan, B.; Mehmood, C. A.; Tareen, N.; Din, W.; Farid, U.; Haider, A. A Survey on Waste Heat Recovery: Electric Power Generation and Potential Prospects within Pakistan. *Renew. Sustain. Energy Rev.* **2017**, *75* (November 2016), 1142–1155.
<https://doi.org/10.1016/j.rser.2016.11.096>.
- (11) Davids, P. S.; Kirsch, J.; Starbuck, A.; Jarecki, R.; Shank, J.; Peters, D. Electrical Power Generation from Moderate-Temperature Radiative Thermal Sources. *Science* **2020**, *1345* (March), 1341–1345. <https://doi.org/10.1126/science.aba2089>.
- (12) Gao, C.; Lee, S. W.; Yang, Y. Thermally Regenerative Electrochemical Cycle for Low-Grade Heat Harvesting. *ACS Energy Lett.* **2017**, *2* (10), 2326–2334.
<https://doi.org/10.1021/acsenergylett.7b00568>.

- (13) Salazar, P. F.; Kumar, S.; Cola, B. A. Design and Optimization of Thermo-Electrochemical Cells. *J. Appl. Electrochem.* **2014**, *44* (2), 325–336. <https://doi.org/10.1007/s10800-013-0638-y>.
- (14) Cheng-Gong Han, Xin Qian, Qikai Li, Biao Deng, Yongbin Zhu, Zhijia Han, Wenqing Zhang, Weichao Wang, Shien-Ping Feng, Gang Chen, W. L. Giant Thermopower of Ionic Gelatin near Room Temperature. *Science (80-.)*. **2020**, *5045* (February 2019), 1–13.
- (15) Kim, J. H.; Lee, J. H.; Palem, R. R.; Suh, M. S.; Lee, H. H.; Kang, T. J. Iron (II/III) Perchlorate Electrolytes for Electrochemically Harvesting Low-Grade Thermal Energy. *Sci. Rep.* **2019**, *9* (1), 1–8. <https://doi.org/10.1038/s41598-019-45127-w>.
- (16) Pennelli, G. Review of Nanostructured Devices for Thermoelectric Applications. *Beilstein J. Nanotechnol.* **2014**, *5* (1), 1268–1284. <https://doi.org/10.3762/bjnano.5.141>.
- (17) Abraham, T. J.; Macfarlane, D. R.; Baughman, R. H.; Jin, L.; Li, N.; Pringle, J. M. Towards Ionic Liquid-Based Thermoelectrochemical Cells for the Harvesting of Thermal Energy. *Electrochim. Acta* **2013**, *113*, 87–93. <https://doi.org/10.1016/j.electacta.2013.08.087>.
- (18) Liu, W.; Jie, Q.; Kim, H. S.; Ren, Z. Current Progress and Future Challenges in Thermoelectric Power Generation: From Materials to Devices. *Acta Mater.* **2015**, *87* (155), 357–376. <https://doi.org/10.1016/j.actamat.2014.12.042>.
- (19) Hu, R.; Cola, B. A.; Haram, N.; Barisci, J. N.; Lee, S.; Stoughton, S.; Wallace, G.; Too, C.; Thomas, M.; Gestos, A.; Dela Cruz, M. E.; Ferraris, J. P.; Zakhidov, A. A.; Baughman, R. H. Harvesting Waste Thermal Energy Using a Carbon-Nanotube-Based Thermo-Electrochemical Cell. *Nano Lett.* **2010**, *10* (3), 838–846.

<https://doi.org/10.1021/nl903267n>.

- (20) Quickenden, T. I. A Review of Power Generation in Aqueous Thermogalvanic Cells. *J. Electrochem. Soc.* **1995**, *142* (11), 3985. <https://doi.org/10.1149/1.2048446>.
- (21) Zhang, L.; Kim, T.; Li, N.; Kang, T. J.; Chen, J.; Pringle, J. M.; Zhang, M.; Kazim, A. H.; Fang, S.; Haines, C.; Al-Masri, D.; Cola, B. A.; Razal, J. M.; Di, J.; Beirne, S.; MacFarlane, D. R.; Gonzalez-Martin, A.; Mathew, S.; Kim, Y. H.; Wallace, G.; Baughman, R. H. High Power Density Electrochemical Thermocells for Inexpensively Harvesting Low-Grade Thermal Energy. *Adv. Mater.* **2017**, *29* (12), 1–7. <https://doi.org/10.1002/adma.201605652>.
- (22) Abraham, T. J.; MacFarlane, D. R.; Pringle, J. M. Seebeck Coefficients in Ionic Liquids - Prospects for Thermo-Electrochemical Cells. *Chem. Commun.* **2011**, *47* (22), 6260–6262. <https://doi.org/10.1039/c1cc11501d>.
- (23) Sosnowska, A.; Barycki, M.; Gajewicz, A.; Bobrowski, M.; Freza, S.; Skurski, P.; Uhl, S.; Laux, E.; Journot, T.; Jeandupeux, L.; Keppner, H.; Puzyn, T. Towards the Application of Structure–Property Relationship Modeling in Materials Science: Predicting the Seebeck Coefficient for Ionic Liquid/Redox Couple Systems. *ChemPhysChem* **2016**, 1591–1600. <https://doi.org/10.1002/cphc.201600080>.
- (24) He, J.; Al-Masri, D.; MacFarlane, D. R.; Pringle, J. M. Temperature Dependence of the Electrode Potential of a Cobalt-Based Redox Couple in Ionic Liquid Electrolytes for Thermal Energy Harvesting. *Faraday Discuss.* **2016**, *190*, 205–218. <https://doi.org/10.1039/c5fd00238a>.
- (25) Kang, T. J.; Fang, S.; Kozlov, M. E.; Haines, C. S.; Li, N.; Kim, Y. H.; Chen, Y.;

- Baughman, R. H. Electrical Power from Nanotube and Graphene Electrochemical Thermal Energy Harvesters. *Adv. Funct. Mater.* **2012**, *22* (3), 477–489. <https://doi.org/10.1002/adfm.201101639>.
- (26) Duan, J.; Feng, G.; Liu, K.; Zhou, J.; Yu, B.; Li, J.; Chen, M. Aqueous Thermogavanic Cells with a High Seebeck Coefficient for Low-Grade Heat Harvest. *Nat. Commun.* **2018**, *9*, 1–8. <https://doi.org/10.1038/s41467-018-07625-9>.
- (27) Yu, B.; Duan, J.; Cong, H.; Xie, W.; Liu, R.; Zhuang, X.; Wang, H.; Qi, B.; Xu, M.; Wang, Z. L.; Zhou, J. Thermosensitive Crystallization–Boosted Liquid Thermocells for Low-Grade Heat Harvesting. *Science* (80-.). **2020**, *346* (October), eabd6749. <https://doi.org/10.1126/science.abd6749>.
- (28) Huang, B.; Muy, S.; Feng, S.; Katayama, Y.; Lu, Y. C.; Chen, G.; Shao-Horn, Y. Non-Covalent Interactions in Electrochemical Reactions and Implications in Clean Energy Applications. *Phys. Chem. Chem. Phys.* **2018**, *20* (23), 15680–15686. <https://doi.org/10.1039/c8cp02512f>.
- (29) Al-Masri, D.; Dupont, M.; Yunis, R.; MacFarlane, D. R.; Pringle, J. M. The Electrochemistry and Performance of Cobalt-Based Redox Couples for Thermoelectrochemical Cells. *Electrochim. Acta* **2018**, *269*, 714–723. <https://doi.org/10.1016/j.electacta.2018.03.032>.
- (30) Lazar, M. A.; Al-Masri, D.; Macfarlane, D. R.; Pringle, J. M. Enhanced Thermal Energy Harvesting Performance of a Cobalt Redox Couple in Ionic Liquid-Solvent Mixtures. *Phys. Chem. Chem. Phys.* **2016**, *18* (3), 1404–1410. <https://doi.org/10.1039/c5cp04305k>.
- (31) Taheri, A.; MacFarlane, D. R.; Pozo-Gonzalo, C.; Pringle, J. M. Application of a Water-

- Soluble Cobalt Redox Couple in Free-Standing Cellulose Films for Thermal Energy Harvesting. *Electrochim. Acta* **2019**, *297*, 669–675. <https://doi.org/10.1016/j.electacta.2018.11.208>.
- (32) Laux, E.; Uhl, S.; Journot, T.; Brossard, J.; Jeandupeux, L.; Keppner, H. Aspects of Protonic Ionic Liquid as Electrolyte in Thermoelectric Generators. *J. Electron. Mater.* **2016**, *45* (7), 3383–3389. <https://doi.org/10.1007/s11664-016-4526-1>.
- (33) Burmistrov, I.; Kovyneva, N.; Gorshkov, N.; Gorokhovskiy, A.; Durakov, A. Development of New Electrode Materials for Thermo-Electrochemical Cells for Waste Heat Harvesting. *Reinf. Plast.* **2019**, *29* (June), 42–48. <https://doi.org/10.1016/j.ref.2019.02.003>.
- (34) Kim, J. H.; Kang, T. J. Diffusion and Current Generation in Porous Electrodes for Thermo-Electrochemical Cells. *ACS Appl. Mater. Interfaces* **2019**, *11* (32), 28894–28899. <https://doi.org/10.1021/acsami.9b08381>.
- (35) Im, H.; Kim, T.; Song, H.; Choi, J.; Park, J. S.; Ovalle-Robles, R.; Yang, H. D.; Kihm, K. D.; Baughman, R. H.; Lee, H. H.; Kang, T. J.; Kim, Y. H. High-Efficiency Electrochemical Thermal Energy Harvester Using Carbon Nanotube Aerogel Sheet Electrodes. *Nat. Commun.* **2016**, *7*, 1–9. <https://doi.org/10.1038/ncomms10600>.
- (36) Romano, M. S.; Li, N.; Antiohos, D.; Razal, J. M.; Nattestad, A.; Beirne, S.; Fang, S.; Chen, Y.; Jalili, R.; Wallace, G. G.; Baughman, R.; Chen, J. Carbon Nanotube-Reduced Graphene Oxide Composites for Thermal Energy Harvesting Applications. *Adv. Mater.* **2013**, *25* (45), 6602–6606. <https://doi.org/10.1002/adma.201303295>.
- (37) Yang, P.; Liu, K.; Chen, Q.; Mo, X.; Zhou, Y.; Li, S.; Feng, G.; Zhou, J. Wearable

- Thermocells Based on Gel Electrolytes for the Utilization of Body Heat. *Angew. Chemie - Int. Ed.* **2016**, *55* (39), 12050–12053. <https://doi.org/10.1002/anie.201606314>.
- (38) Lee, S. W.; Yang, Y.; Lee, H. W.; Ghasemi, H.; Kraemer, D.; Chen, G.; Cui, Y. An Electrochemical System for Efficiently Harvesting Low-Grade Heat Energy. *Nat. Commun.* **2014**, *5* (May), 1–6. <https://doi.org/10.1038/ncomms4942>.
- (39) Chen, R.; Deng, S.; Xu, W.; Zhao, L. A Graphic Analysis Method of Electrochemical Systems for Low-Grade Heat Harvesting from a Perspective of Thermodynamic Cycles. *Energy* **2020**, *191*, 116547. <https://doi.org/10.1016/j.energy.2019.116547>.
- (40) Rahimi, M.; Straub, A. P.; Zhang, F.; Zhu, X.; Elimelech, M.; Gorski, C. A.; Logan, B. E. Emerging Electrochemical and Membrane-Based Systems to Convert Low-Grade Heat to Electricity. *Energy Environ. Sci.* **2018**, *11* (2), 276–285. <https://doi.org/10.1039/c7ee03026f>.
- (41) Yang, Y.; Loomis, J.; Ghasemi, H.; Lee, S. W.; Wang, Y. J.; Cui, Y.; Chen, G. Membrane-Free Battery for Harvesting Low-Grade Thermal Energy. *Nano Lett.* **2014**, *14* (11), 6578–6583. <https://doi.org/10.1021/nl5032106>.
- (42) Yang, Y.; Lee, S. W.; Ghasemi, H.; Loomis, J.; Li, X.; Kraemer, D.; Zheng, G.; Cui, Y.; Chen, G. Charging-Free Electrochemical System for Harvesting Low-Grade Thermal Energy. *Proc. Natl. Acad. Sci. U. S. A.* **2014**, *111* (48), 17011–17016. <https://doi.org/10.1073/pnas.1415097111>.
- (43) Ding, Y.; Guo, X.; Ramirez-Meyers, K.; Zhou, Y.; Zhang, L.; Zhao, F.; Yu, G. Simultaneous Energy Harvesting and Storage: Via Solar-Driven Regenerative Electrochemical Cycles. *Energy Environ. Sci.* **2019**, *12* (11), 3370–3379.

<https://doi.org/10.1039/c9ee01930h>.

- (44) Zhang, X.; Pan, Y.; Cai, L.; Zhao, Y.; Chen, J. Using Electrochemical Cycles to Efficiently Exploit the Waste Heat from a Proton Exchange Membrane Fuel Cell. *Energy Convers. Manag.* **2017**, *144*, 217–223. <https://doi.org/10.1016/j.enconman.2017.04.058>.
- (45) Shapira, B.; Cohen, I.; Penki, T. R.; Avraham, E.; Aurbach, D. Energy Extraction and Water Treatment in One System: The Idea of Using a Desalination Battery in a Cooling Tower. *J. Power Sources* **2018**, *378* (October 2017), 146–152. <https://doi.org/10.1016/j.jpowsour.2017.12.039>.
- (46) Jiang, J.; Tian, H.; He, X.; Zeng, Q.; Niu, Y.; Zhou, T.; Yang, Y.; Wang, C. A CoHCF System with Enhanced Energy Conversion Efficiency for Low-Grade Heat Harvesting. *J. Mater. Chem. A* **2019**, *7* (41), 23862–23867. <https://doi.org/10.1039/c9ta02426c>.
- (47) Liu, Y.; Gao, C.; Sim, S.; Kim, M.; Lee, S. W. Lithium Manganese Oxide in an Aqueous Electrochemical System for Low-Grade Thermal Energy Harvesting. *Chem. Mater.* **2019**, *31* (12), 4379–4384. <https://doi.org/10.1021/acs.chemmater.9b00310>.
- (48) Linford, P. A.; Xu, L.; Huang, B.; Shao-Horn, Y.; Thompson, C. V. Multi-Cell Thermogalvanic Systems for Harvesting Energy from Cyclic Temperature Changes. *J. Power Sources* **2018**, *399* (June), 429–435. <https://doi.org/10.1016/j.jpowsour.2018.07.080>.
- (49) Wang, Y.; Cai, L.; Peng, W.; Zhou, Y.; Chen, J. Maximal Continuous Power Output and Parametric Optimum Design of an Electrochemical System Driven by Low-Grade Heat. *Energy Convers. Manag.* **2017**, *138*, 156–161. <https://doi.org/10.1016/j.enconman.2017.01.045>.

- (50) Long, R.; Li, B.; Liu, Z.; Liu, W. Performance Analysis of a Thermally Regenerative Electrochemical Cycle for Harvesting Waste Heat. *Energy* **2015**, *87*, 463–469. <https://doi.org/10.1016/j.energy.2015.05.016>.
- (51) Guo, J.; Wang, Y.; Gonzalez-Ayala, J.; Roco, J. M. M.; Medina, A.; Calvo Hernández, A. Continuous Power Output Criteria and Optimum Operation Strategies of an Upgraded Thermally Regenerative Electrochemical Cycles System. *Energy Convers. Manag.* **2019**, *180* (June 2018), 654–664. <https://doi.org/10.1016/j.enconman.2018.11.024>.
- (52) Li, L.; Kim, S.; Wang, W.; Vijayakumar, M.; Nie, Z.; Chen, B.; Zhang, J.; Xia, G.; Hu, J.; Graff, G.; Liu, J.; Yang, Z. A Stable Vanadium Redox-Flow Battery with High Energy Density for Large-Scale Energy Storage. *Adv. Energy Mater.* **2011**, *1* (3), 394–400. <https://doi.org/10.1002/aenm.201100008>.
- (53) Eapen, D. E.; Choudhury, S. R.; Rengaswamy, R. Low Grade Heat Recovery for Power Generation through Electrochemical Route: Vanadium Redox Flow Battery, a Case Study. *Appl. Surf. Sci.* **2019**, *474*, 262–268. <https://doi.org/10.1016/j.apsusc.2018.02.025>.
- (54) Reynard, D.; Dennison, C. R.; Battistel, A.; Girault, H. H. Efficiency Improvement of an All-Vanadium Redox Flow Battery by Harvesting Low-Grade Heat. *J. Power Sources* **2018**, *390* (March), 30–37. <https://doi.org/10.1016/j.jpowsour.2018.03.074>.
- (55) Chow, T. T. A Review on Photovoltaic/Thermal Hybrid Solar Technology. *Appl. Energy* **2010**, *87* (2), 365–379. <https://doi.org/10.1016/j.apenergy.2009.06.037>.
- (56) Skyllas-Kazacos, M.; Cao, L.; Kazacos, M.; Kausar, N.; Mousa, A. Vanadium Electrolyte Studies for the Vanadium Redox Battery—A Review. *ChemSusChem* **2016**, *9* (13), 1521–1543. <https://doi.org/10.1002/cssc.201600102>.

- (57) Zhang, C.; Zhao, T. S.; Xu, Q.; An, L.; Zhao, G. Effects of Operating Temperature on the Performance of Vanadium Redox Flow Batteries. *Appl. Energy* **2015**, *155*, 349–353. <https://doi.org/10.1016/j.apenergy.2015.06.002>.
- (58) Poletayev, A. D.; McKay, I. S.; Chueh, W. C.; Majumdar, A. Continuous Electrochemical Heat Engines. *Energy Environ. Sci.* **2018**, *11* (10), 2964–2971. <https://doi.org/10.1039/c8ee01137k>.
- (59) Peljo, P.; Lloyd, D.; Doan, N.; Majaneva, M.; Kontturi, K. Towards a Thermally Regenerative All-Copper Redox Flow Battery. *Phys. Chem. Chem. Phys.* **2014**, *16* (7), 2831–2835. <https://doi.org/10.1039/c3cp54585g>.
- (60) Zhang, F.; Liu, J.; Yang, W.; Logan, B. E. A Thermally Regenerative Ammonia-Based Battery for Efficient Harvesting of Low-Grade Thermal Energy as Electrical Power. *Energy Environ. Sci.* **2015**, *8* (1), 343–349. <https://doi.org/10.1039/c4ee02824d>.
- (61) Rahimi, M.; Zhu, L.; Kowalski, K. L.; Zhu, X.; Gorski, C. A.; Hickner, M. A.; Logan, B. E. Improved Electrical Power Production of Thermally Regenerative Batteries Using a Poly(Phenylene Oxide) Based Anion Exchange Membrane. *J. Power Sources* **2017**, *342*, 956–963. <https://doi.org/10.1016/j.jpowsour.2017.01.003>.
- (62) Rahimi, M.; D'Angelo, A.; Gorski, C. A.; Scialdone, O.; Logan, B. E. Electrical Power Production from Low-Grade Waste Heat Using a Thermally Regenerative Ethylenediamine Battery. *J. Power Sources* **2017**, *351*, 45–50. <https://doi.org/10.1016/j.jpowsour.2017.03.074>.
- (63) Rahimi, M.; Kim, T.; Gorski, C. A.; Logan, B. E. MWA Thermally Regenerative Ammonia Battery with Carbon-Silver Electrodes for Converting Low-Grade Waste Heat

- to Electricity. *J. Power Sources* **2018**, 373 (November 2017), 95–102.
<https://doi.org/10.1016/j.jpowsour.2017.10.089>.
- (64) Wang, W.; Shu, G.; Tian, H.; Zhu, X. A Numerical Model for a Thermally-Regenerative Ammonia-Based Flow Battery Using for Low Grade Waste Heat Recovery. *J. Power Sources* **2018**, 388 (November 2017), 32–44.
<https://doi.org/10.1016/j.jpowsour.2018.03.070>.
- (65) Zhang, F.; LaBarge, N.; Yang, W.; Liu, J.; Logan, B. E. Enhancing Low-Grade Thermal Energy Recovery in a Thermally Regenerative Ammonia Battery Using Elevated Temperatures. *ChemSusChem* **2015**, 8 (6), 1043–1048.
<https://doi.org/10.1002/cssc.201403290>.
- (66) Wang, W.; Tian, H.; Shu, G.; Huo, D.; Zhang, F.; Zhu, X. A Bimetallic Thermally Regenerative Ammonia-Based Battery for High Power Density and Efficiently Harvesting Low-Grade Thermal Energy. *J. Mater. Chem. A* **2019**, 7 (11), 5991–6000.
<https://doi.org/10.1039/c8ta10257k>.
- (67) Sales, B. B.; Burheim, O. S.; Porada, S.; Presser, V.; Buisman, C. J. N.; Hamelers, H. V. M. Extraction of Energy from Small Thermal Differences near Room Temperature Using Capacitive Membrane Technology. *Environ. Sci. Technol. Lett.* **2014**, 1 (9), 356–360.
<https://doi.org/10.1021/ez5002402>.
- (68) Härtel, A.; Janssen, M.; Weingarh, D.; Presser, V.; Van Rooij, R. Heat-to-Current Conversion of Low-Grade Heat from a Thermocapacitive Cycle by Supercapacitors. *Energy Environ. Sci.* **2015**, 8 (8), 2396–2401. <https://doi.org/10.1039/c5ee01192b>.
- (69) Wang, X.; Huang, Y. T.; Liu, C.; Mu, K.; Li, K. H.; Wang, S.; Yang, Y.; Wang, L.; Su,

- C. H.; Feng, S. P. Direct Thermal Charging Cell for Converting Low-Grade Heat to Electricity. *Nat. Commun.* **2019**, *10* (1), 1–8. <https://doi.org/10.1038/s41467-019-12144-2>.
- (70) Straub, A. P.; Yip, N. Y.; Lin, S.; Lee, J.; Elimelech, M. Harvesting Low-Grade Heat Energy Using Thermo-Osmotic Vapour Transport through Nanoporous Membranes. *Nat. Energy* **2016**, *1* (7). <https://doi.org/10.1038/nenergy.2016.90>.
- (71) Straub, A. P.; Elimelech, M. Energy Efficiency and Performance Limiting Effects in Thermo-Osmotic Energy Conversion from Low-Grade Heat. *Environ. Sci. Technol.* **2017**, *51* (21), 12925–12937. <https://doi.org/10.1021/acs.est.7b02213>.
- (72) Phillip, W. A. Thermal-Energy Conversion: Under Pressure. *Nat. Energy* **2016**, *1* (7), 10–11. <https://doi.org/10.1038/nenergy.2016.101>.
- (73) Xie, G.; Li, P.; Zhang, Z.; Xiao, K.; Kong, X. Y.; Wen, L.; Jiang, L. Skin-Inspired Low-Grade Heat Energy Harvesting Using Directed Ionic Flow through Conical Nanochannels. *Adv. Energy Mater.* **2018**, *8* (22), 1–6. <https://doi.org/10.1002/aenm.201800459>.
- (74) Liu, G.; Chen, T.; Xu, J.; Li, G.; Wang, K. Solar Evaporation for Simultaneous Steam and Power Generation. *J. Mater. Chem. A* **2020**, *8* (2), 513–531. <https://doi.org/10.1039/c9ta12211g>.
- (75) Cheng, Q.; Fan, W.; He, Y.; Ma, P.; Vanka, S.; Fan, S.; Mi, Z.; Wang, D. Photorechargeable High Voltage Redox Battery Enabled by Ta₃N₅ and GaN/Si Dual-Photoelectrode. *Adv. Mater.* **2017**, *29* (26), 1–8. <https://doi.org/10.1002/adma.201700312>.
- (76) Yang, Y.; Zhang, H.; Zhu, G.; Lee, S.; Lin, Z. H.; Wang, Z. L. Flexible Hybrid Energy Cell for Simultaneously Harvesting Thermal, Mechanical, and Solar Energies. *ACS Nano*

- 2013**, 7 (1), 785–790. <https://doi.org/10.1021/nn305247x>.
- (77) Anari, E. H. B.; Romano, M.; Teh, W. X.; Black, J. J.; Jiang, E.; Chen, J.; To, T. Q.; Panchompoo, J.; Aldous, L. Substituted Ferrocenes and Iodine as Synergistic Thermoelectrochemical Heat Harvesting Redox Couples in Ionic Liquids. *Chem. Commun.* **2016**, 52 (4), 745–748. <https://doi.org/10.1039/c5cc05889a>.
- (78) Zhu, X.; Rahimi, M.; Gorski, C. A.; Logan, B. A Thermally-Regenerative Ammonia-Based Flow Battery for Electrical Energy Recovery from Waste Heat. *ChemSusChem* **2016**, 9 (8), 873–879. <https://doi.org/10.1002/cssc.201501513>.